This article has been accepted for publication in IEEE Internet of Things Journal. This is the author's version which has not been fully edited and content may change prior to final publication. Citation information: DOI 10.1109/JIOT.2023.3305610

Consensus Based Distributed Collective Motion of Swarm of Quadcopters

Solomon Gudeta, Ali Karimoddini, and Negasa Yahi

***Abstract*—This paper presents a scalable hierarchical distributed control framework to address the problem of collective navigation of a quadcopter swarm, which is a special form of Internet of Vehicles (IoV), in the presence of member drop-outs and inter-robot communication link failures. The proposed control framework has three parts: the swarm descriptors (the geometric interpretation of swarm statistics) estimator, the cooperative swarm motion controller, and the attitude controller. The proposed framework includes a novel distributed dynamic average consensus algorithm to estimate the swarm descriptors which represent the collective motion of the swarm in the abstract space (a lower dimensional space independent of number and permutation of robots in the swarm). By employing a dynamic inversion approach, in the cooperative swarm motion controller, we design a control law that generates the desired thrust, yaw, pitch, and roll angle commands. In the attitude controller, we convert the desired commands from the cooperative swarm motion controller into the rolling, pitching, and yawing moments required to realize the collective motion of the swarm. The robustness of the proposed framework and the stability of the proposed swarm descriptors estimator, the cooperative swarm motion controller, and the attitude controller, and the overall cascaded system are mathematically proved. The significance of the proposed control framework is demonstrated via simulation in the presence of member robot drop-outs and inter-robot communication link failures.**

***Index Terms*—Swarm, Quadcopter, Internet of Vehicles, Collective Motion, Cyber-Physical Systems, Vehicular Networks, IoT Application Platforms**

I. Introduction

During the last decades, a significant amount of attention has been given to the coordinated collective motion of Internet of Vehicles (IoV) to perform tasks that are too risky for humans, or where fast response is crucial, and beyond the capabilities of a single or few individuals. There has been a growing body of research [1]–[5] extending formation control of multi-agents and platooning of Connected and Automated Vehicles (CAVs), among other topics, to swarm of CAVs. The conventional CAV control systems mainly focus on highway vehicles and related concerns, such as platoon driving, coordinated driving in multiple lanes, and management of multi-lane intersections [5]–[8].In [3], a distance based formation control has been extended to realize multi-lane platooning. Further, with the advancements in Vehicle-to-Vehicle (V2V) communication and shared perception techniques, it has become viable to coordinate a group of autonomous vehicles beyond field-of-view to efficiently complete complex missions within unstructured environment. An example is the coordination of the swarm of quadcopters that are capable of efficiently performing collaborative tasks beyond visual and communication line-of-sight.

The authors in [9]–[11], developed swarms of quadcopters that are convenient for various applications such as agricultural spraying, pollination, monitoring, and collection of aerial imagery in an efficient way. In [12]–[15], the authors developed swarm systems that can perform collaborative localization, surveillance, load transport, and target tracking. In general, the capability of robotic swarms to efficiently and effectively complete various complex tasks emanates from the inherent characteristics of swarm robotic systems such as redundancy, simplicity, low cost, and the ability to generate complex global behaviors from local interactions [16], [17]. However, the relative simplicity in design and size of individual swarm members may inherently limit their sensing, actuation, communication, computation, and performance capabilities. Therefore, the guidance and control algorithms of a swarm should be required to be computationally efficient, scalable to varying numbers of robots, and robust to V2V communication loss between adjacent robots. Accordingly, a coordinated collective motion of swarm of quadcopters creates exciting and challenging control problems due to the competing requirements and the complicated quadcopter dynamics.

Based on feedback linearization and consensus theory, the formation control of a swarm of quadcopters is proposed in [18] for a time-invariant formation case. The coordinated collective motion based on nonlinear model of quadcopters were addressed in [19] and [20]. In [21]–[23], ignoring the rotational dynamics of each robots, multi-robot formation control frameworks are proposed for a team of UAVs. Further, more unified coordinated collective motion frameworks that consider the translational and rotational motions of a team of quadcopters were studied in [24]–[27] for simplified models of quadcopter dynamics. Modeling a quadcopter as a six degrees of freedom (6-DOF) under-actuated system, the authors in [28] proposed a leader-follower-based collective flight control of a group of quadcopters in which each follower knows the position of the leader robot. Recently, in [29], a consensus-based robust formation control approach is proposed for a group of quadcopters with full nonlinear dynamics in the presence of motion disturbances. The aforementioned consensus-based approaches mainly ignore or simplify the quadcopter dynamics and require each robot in the swarm to be provided with unique specifications of formation parameters. Hence, the swarm's collective navigation performance is limited and does

All the authors are with the Department of Electrical and Computer Engineering, North Carolina Agricultural and Technical State University, Greensboro, North Carolina, USA.

Corresponding author: A. Karimoddini, Tel: +13362853313, akarimod@ncat.edu.

not scale to a varying number of robots in the group.

Our aim in this paper is to develop a scalable control algorithm for swarm quadcopters to realize collective motion of the swarm. In this vein, the authors in [30], proposed a control framework by encoding the coordinated collective motion of the swarm using a finite number of swarm descriptors to navigate the swarm along the desired path. The swarm descriptors are extracted from the statistics of the swarm's distribution. In [31], a control framework to steer a swarm of robots is proposed based on the mean and covariance of the swarm's distribution and hysteresis-based switching technique. Extending the work in [30], the authors in [32] proposed a control law to manipulate objects by a group of robots. However, the frameworks proposed in [30]–[32] are based on a centralized communication architecture. Alternatively, in [33]–[35] a swarm control framework based on the local sensing inputs and information from the neighboring robots is developed. The local controller on each robot chooses a control action that minimizes a global cost that describes the deviation of the actual collective motion of the swarm from the desired values. However, the performance of the framework proposed in [33], [34] deteriorates for time-varying swarm formation. The framework proposed in [33], [34] is extended in [36] by decoupling the local estimators from the local controllers on robots. Decoupling the local estimators from the controllers equips the framework to avoid large estimation [37] and formation errors in time and improves the performance of coordinated motion of robotic swarms. However, the proposed framework suffers from the change in the communication topology that arises from robot drop-outs and communication link failures among adjacent robots. Therefore, there is a need to design a scalable and robust control framework for collective navigation of swarm of quadcopters in the presence of varying number of members, varying topology, and varying inter-UAV distances.

This paper introduces a hierarchical distributed control framework for collective navigation of swarm of quadcopters under undirected communication topologies subjected to member robot drop-outs and communication link failures among adjacent robots. The proposed framework consists of a cooperative motion controller to govern the motion of the whole group, and an attitude controller to stabilize the rotational dynamics of a particular quadcopter. The main features of the proposed framework are synopsized as follows. First, the proposed control framework allows the swarm to perform a time-varying collective scaling, translation, and rotation. Second, the proposed framework is robust to robot drop-outs and communication link failures between adjacent robots due to decoupling of the estimation of the swarm descriptors from the swarm control.

Compared to the previous related works, the contributions of this paper are summarized as follows:

1) This paper develops a scalable control framework – independent of a varying number of robots in the swarm– for collective navigation of swarm of quadcopters. To this end, in our case, all the robots in the swarm are given the same formation parameters. Our formation parameters are global swarm descriptors such as the swarm's center, attitude, width, length, and height. These formation parameters capture a swarm's global description, unlike the formation parameters discussed in state-of-the-art. For example, the approaches considered in [27], [29], [38], [39] requires unique formation parameters for each individual robot in the swarm. However, rather than specifying unique formation parameters for each individual robot, in our proposed framework, we only provide the same formation parameters for each robot in the swarm. Further, the proposed control framework is also independent of the number of and permutations of robots in the swarm.
2) The proposed framework in this paper is robust to robot drop-outs and loss of communication between adjacent robots in the swarm. Compared to the work in [30]–[32], the proposed framework does not require a centralized observer moving with the swarm as the observer failure leads to the whole swarm failure.
3) This paper develops a distributed and hierarchical high-performance collective navigation of a swarm of quadcopters. Unlike the approaches in [24]–[27], [38], [39], we do not ignore or simplify the quadcopter dynamics as the accurate model of the quadcopter is crucial to realize time-varying coordinated motions with aggressive maneuvers. Further, we separate the group motion control, the estimation of the swarm descriptor, and the low-level control from each other. This is very useful in analyzing the stability of the collective navigation of the swarm mathematically.

We organize the rest of this paper as follows. In Section II, we present the preliminaries on the graph theory to model the UAV swarm communication network. Also, the modelling of quadcopter dynamics, abstraction of swarm dynamics and the problem formulation are presented in Section II. Section III details the development of consensus-based distributed collective motion framework for UAV swarms. In Section IV, we discuss the detailed stability and convergence analysis of the developed framework. In Section V, the flight simulation results are presented to evaluate and demonstrate the effectiveness of the proposed consensus-based distributed collective motion framework. Concluding remarks are synopsized in Section VI.

II. Preliminaries, Notation and Problem Formulation

A. Graph theory

In this paper, we employ the following notations and basic concepts from graph theory to present the proposed control framework for the collective navigation of swarms of UAVs. Let $\mathcal{G}(t) = (\mathcal{V}(t), \mathcal{E}(t))$ be a graph with N nodes at time instant t, where $\mathcal{V}(t) \triangleq \{v_1(t), \cdots, v_N(t)\}$ is the set of nodes and $\mathcal{E}(t) \subseteq \mathcal{V}(t) \times \mathcal{V}(t)$–$\{(v_i(t), v_i(t))|v_i(t) \in \mathcal{V}(t)\}$ is the set of edges. Let $\mathcal{A}(t) = [\mathcal{A}_{ij}(t)] \in \mathbb{R}^{N\times N}$ be the adjacency matrix where $i, j \in \{1, 2, \cdots, N\}$, $\mathcal{A}_{ij}(t) = 1$ if there exists an edge from node i to node j, and $\mathcal{A}_{ij}(t) = 0$, otherwise. Here, we assume that $\mathcal{G}$ is bidirectional, i.e., $\mathcal{A}_{ij}(t) = \mathcal{A}_{ji}(t)$

Notation	Description
$\mathcal{G}(t)$	Swarm commucation graph
$\mathcal{V}(t)$	Set of nodes in $\mathcal{G}(t)$
$\mathcal{E}(t))$	Set of edges in $\mathcal{G}(t)$
$\mathcal{B}(t)$	Incidence matrix of $\mathcal{G}(t)$
$\mathcal{L}(t)$	Laplacian matrix of $\mathcal{G}(t)$
$\lambda_2(\mathcal{L}(t))$	the algebraic connectivity of $\mathcal{G}(t)$
$\lambda_{max}(\mathcal{L}(t))$	the maximum eigenvalue of $\mathcal{L}(t)$
$\Delta(t)$	Degree matrix of $\mathcal{G}(t)$
$\mathcal{A}(t)$	Adjacency matrix of $\mathcal{G}(t)$
$\mathcal{N}_i(t)$	Set of Robot i neighbors in $\mathcal{G}(t)$
$\mathbf{1}_N$	$N-$dimensional vector of all ones
I_N	$N \times N$ identity matrix
M	$I_N - \frac{\mathbf{1}_N \mathbf{1}_N^{\mathrm{T}}}{N}$
$(.)^+$	generalized inverse
$\|.\|_1$	$1-$norm
$\|.\|_2$	$2-$norm
$\|.\|_\infty$	$\infty-$norm
$\mathcal{K}_\infty$	Class kappa function
$SO(3)$	Special Orthogonal Group

TABLE I: Notations

for all $i, j \in \{1, 2, \cdots, N\}$. We consider the set of neighbors $\mathcal{N}_i(t)$ of node v_i as

$$\mathcal{N}_i(t) = \{v_j \in \mathcal{V}(t) : \mathcal{A}_{ij}(t) = 1\}. \tag{1}$$

For a bidirectional graph, the out degree of node v_i is given as $d_i(t) = \sum_{j=1}^{N} \mathcal{A}_{ij}(t)$. Then, the degree matrix and the Laplacian matrix of graph $\mathcal{G}(t)$ is given by $\Delta(t) = \text{diag}(d_i(t))$ and $\mathcal{L}(t) = \Delta(t) - \mathcal{A}(t)$, respectively. More specifically, $\mathcal{L}(t) = [l_{ij}(t)] \in \mathbb{R}^{N \times N}$, where $l_{ii}(t) = \sum_{j=1}^{N} \mathcal{A}_{ij}(t)$ and $l_{ij}(t) = -\mathcal{A}_{ij}(t)$ if $i \neq j$. The incidence matrix of graph $\mathcal{G}(t)$ is given by $\mathcal{B}(t) = [b_{ij}(t)] \in \{-1, 0, 1\}^{N \times k}$, where $b_{ij}(t) = -1$ for the outgoing communication link from node i, $b_{ij}(t) = 1$ for the incoming communication link to node i, and $b_{ij}(t) = 0$ otherwise. Here, k is the total number of edges in the graph which can be calculated as $k = \sum_{i=1}^{N} d_i(t)$. For ease of access, the notations related to graph theory is summarized in Table I. Further, we present the following two lemmas which will be used in the next sections.

Lemma 1 ([40]). *For any strongly connected bidirectional graph $\mathcal{G}(t)$, the Laplacian matrix $\mathcal{L}(t)$ and the incidence matrix $\mathcal{B}(t)$ satisfy $M = \mathcal{L}(t)(\mathcal{L}(t))^+ = (\mathcal{B}(t)\mathcal{B}^{\mathrm{T}}(t))(\mathcal{B}(t)\mathcal{B}^{\mathrm{T}}(t))^+$, where $M \triangleq (I_N - \frac{\mathbf{1}_N \mathbf{1}_N^{\mathrm{T}}}{N})$ and $(.)^+$ is the generalized inverse.*

From Lemma 1 it can be seen that the Laplacian matrix $\mathcal{L}(t)$ and the incidence matrix $\mathcal{B}(t)$ of graph $\mathcal{G}(t)$ are related by $\mathcal{L}(t) = \mathcal{B}(t)\mathcal{B}^{\mathrm{T}}(t)$. Here, the notations $\mathbf{1}_N$ denotes $N-$dimensional vector of all ones, I_N denotes $N \times N$ identity matrix.

Lemma 2 ([41]). *The Laplacian matrix of a strongly connected bidirectional graph $\mathcal{G}(t)$ is a positive semi-definite matrix with a single eigenvalue at zero. The right and left eigenvectors of $\mathcal{L}(t)$ corresponding to the zero eigenvalue are $\mathbf{1}_N$ and $\mathbf{1}_N^{\mathrm{T}}$, respectively.*

Lemma 2 describes that $\forall x \in R^N$, $x^{\mathrm{T}}\mathcal{L}(t)x \geq 0$, $\mathbf{1}_N^T \mathcal{L}(t) = 0$, $\mathbf{1}_N^T \mathcal{B}(t) = 0$, $\mathbf{1}_N^T M = 0$, $\mathcal{L}(t)\mathbf{1}_N = 0$, $\mathcal{B}(t)\mathbf{1}_N = 0$ and $M\mathbf{1}_N = 0$, where $M \triangleq (I_N - \frac{\mathbf{1}_N \mathbf{1}_N^{\mathrm{T}}}{N})$.

B. UAV model

In this section, we present the equation of motion of Quadcopter i, $i \in \{1, \cdots, N\}$, based on its rigid body dynamics. For this purpose, we define the Earth-fixed world frame where the basis vectors point in the north, east, and down to the center of earth and a body reference frame fixed at the bary-center of the quadcopter. The rotation matrix $R_i \in SO(3)$ from the body frame to the Earth-fixed world frame is given as

$$R_i = \begin{bmatrix} \cos\theta_i \cos\psi_i & \sin\phi_i \sin\theta_i \cos\psi_i - \cos\phi_i \sin\psi_i & \cos\phi_i \sin\theta_i \cos\psi_i + \sin\phi_i \sin\psi_i \\ \cos\theta_i \sin\psi_i & \sin\phi_i \sin\theta_i \sin\psi_i + \cos\phi_i \cos\psi_i & \cos\phi_i \sin\theta_i \sin\psi_i - \sin\phi_i \cos\psi_i \\ -\sin\theta_i & \sin\phi_i \cos\theta_i & \cos\phi_i \cos\theta_i \end{bmatrix} \tag{2}$$

where the Euler angles $0 \leq \phi_i, \theta_i < \frac{\pi}{2}$, and ψ_i represent the roll, pitch, and yaw angles of Quadcopter i, respectively. Let $\left[x_i, y_i, z_i, \phi_i, \theta_i, \psi_i\right]^{\mathrm{T}}$ be the vector of Quadcopter i's linear and angular positions in the Earth-fixed frame and $\left[u_i, v_i, w_i, p_i, q_i, r_i\right]^{\mathrm{T}}$ be the vector of Quadcopter i's linear and angular velocities in the body fixed frame. Let F_{i_j} and M_{i_j} be the thrust and moment generated by the $j-th$ propeller on quadcopter i, respectively. Then, the control input to quadcopter i is given as

$$\begin{bmatrix} T_i \\ l_i \\ m_i \\ n_i \end{bmatrix} = \begin{bmatrix} F_{i_1} + F_{i_2} + F_{i_3} + F_{i_4} \\ F_{i_1} D - F_{i_3} D \\ F_{i_2} D - F_{i_4} D \\ M_{i_1} - M_{i_2} + M_{i_3} - M_{i_4} \end{bmatrix}, \tag{3}$$

where D is the arm length, T_i is total thrust from all rotors, l_i is the rolling moment, m_i is the pitching moment, and n_i is the yawing moment of quadcopter i. Thrust T_i and yawing moments M_{ij} of the quadcopter i are achieved by varying the rotational speed of propeller motors ω_{i_j} as

$$F_{i_j} = c\omega_{i_j}^2, M_{ij} = aD\omega_{i_j}^2, j = \{1, \cdots, 4\}, \tag{4}$$

where c is the thrust constant, a is the drag constant. Then, neglecting wind effect, the translation motion dynamics of Quadcopter i in the Earth-fixed world frame is given as

$$\begin{bmatrix} \ddot{x}_i \\ \ddot{y}_i \\ \ddot{z}_i \end{bmatrix} = \begin{bmatrix} 0 \\ 0 \\ g \end{bmatrix} + R_i^{\mathrm{T}} \begin{bmatrix} 0 \\ 0 \\ -\frac{T_i}{m} \end{bmatrix}, \tag{5}$$

where g is the acceleration due to gravity and m is the mass of the quadcopter. Ignoring the ground effects, the gyroscopic moments, and assuming the quadrotor's body inertia is significantly bigger than the rotor inertia and quadrotor structure is symmetric, the rotational motion dynamics of Quadcopter i is given as

$$\begin{bmatrix} \dot{p}_i \\ \dot{q}_i \\ \dot{r}_i \end{bmatrix} = \begin{bmatrix} q_i r_i \frac{I_{yy} - I_{zz}}{I_{xx}} \\ p_i r_i \frac{I_{zz} - I_{xx}}{I_{yy}} \\ p_i q_i \frac{I_{xx} - I_{yy}}{I_{zz}} \end{bmatrix} + \begin{bmatrix} \frac{1}{I_{xx}} & 0 & 0 \\ 0 & \frac{1}{I_{yy}} & 0 \\ 0 & 0 & \frac{1}{I_{zz}} \end{bmatrix} \begin{bmatrix} l_i \\ m_i \\ n_i \end{bmatrix}, \tag{6}$$

where I_{xx}, I_{yy}, and I_{zz} are the body inertia of quadcopter i.

This article has been accepted for publication in IEEE Internet of Things Journal. This is the author's version which has not been fully edited and content may change prior to final publication. Citation information: DOI 10.1109/JIOT.2023.3305610

C. Problem formulation

Consider a swarm of N identical quadcopters deployed to execute a collective navigation task in a coordinated manner. Assume that the set of neighbors $\mathcal{N}_i(t)$ of Quadcopter i is given by

$$\mathcal{N}_i(t) = \{j \in \{1, \cdots, N\} : \left\| [x_i, y_i, z_i]^{\mathrm{T}} - [x_j, y_j, z_j]^{\mathrm{T}} \right\| < c_r, j \neq i\}, \quad (7)$$

where $c_r > 0$ is the communication range of Quadcopter i. Given the state $[x_i, y_i, z_i, \phi_i, \theta_i, \psi_i, \ u_i, v_i, w_i, p_i, q_i, r_i]^{\mathrm{T}}$ of Quadcopter i, $i = 1, \cdots, N$, our objective is to design a control framework for the swarm of quadcopters whose overall dynamics is given by

$$\dot{x} = f(x) + G(x)u, \quad (8)$$

where $x = [x_1, y_1, z_1, \phi_1, \theta_1, \psi_1, \cdots, x_N, y_N, z_N, \phi_N, \theta_N, \psi_N]^{\mathrm{T}}$, $u = [T_1, l_1, m_1, n_1, \cdots, T_N, l_N, m_N, n_N]^{\mathrm{T}}$, to collectively move the group along a desired path in the presence of robot drop-outs and communication link failures.

As the dimension of the swarm system in (8) depends on the number of robots in the swarm, directly solving the aforementioned control problem is difficult for a large number of robots. To circumvent this, we reduce the configuration $x_s = [x_1, y_1, z_1, \cdots, x_N, y_N, z_N]^{\mathrm{T}}$ of the swarm to a lower dimensional representation that will be independent of the number and spatial order of quadcopters in the swarm and facilitate commanding the swarm to satisfy specifications given in terms of time-parameterized curves on the lower dimensional manifold. Here, among all possible lower dimensional representations, we are particularly interested in those representations that are invariant to changes in the absolute reference frames, and involve the lower order moments of the spatial distributions of the robots. Let the swarm of quadcopters be initially in a desired swarm configuration. Also, let a reference frame $(O_0 - x_0 y_0 z_0)$ with origin O_0 and basis vectors x_0, y_0, z_0 represent a world frame. Similarly, let a reference frame $(O_1 - x_{s_b} y_{s_b} z_{s_b})$ with origin O_1 fixed at the center of the swarm and basis vectors x_{sb}, y_{sb}, z_{sb} represent a frame moving with the swarm (see Figure 1). Now, we can compute the position of the center of the swarm $\mu \in \mathbb{R}^3$ as the average of the position vectors of UAVs in the world frame $(O_0 - x_0 y_0 z_0)$ as:

$$\mu = [\mu_x, \mu_y, \mu_z]^{\mathrm{T}} = \left[\frac{\sum_{i=1}^N x_i}{N}, \frac{\sum_{i=1}^N y_i}{N}, \frac{\sum_{i=1}^N z_i}{N} \right]^{\mathrm{T}}. \quad (9)$$

Also, in the world frame $(O_0 - x_0 y_0 z_0)$, the covarinace of the swarm distribution is given as:

$$\Sigma_0 = \begin{bmatrix} \sigma_{xx} & \sigma_{xy} & \sigma_{xz} \\ \sigma_{xy} & \sigma_{yy} & \sigma_{yz} \\ \sigma_{xz} & \sigma_{yz} & \sigma_{zz} \end{bmatrix}, \quad (10)$$

where $\sigma_{xx} = \frac{\sum_{i=1}^N (x_i - \mu_x)^2}{N}$, $\sigma_{xy} = \frac{\sum_{i=1}^N (x_i - \mu_x)(y_i - \mu_y)}{N}$, $\sigma_{xz} = \frac{\sum_{i=1}^N (x_i - \mu_x)(z_i - \mu_z)}{N}$, $\sigma_{yy} = \frac{\sum_{i=1}^N (y_i - \mu_y)^2}{N}$, $\sigma_{yz} = \frac{\sum_{i=1}^N (y_i - \mu_y)(z_i - \mu_z)}{N}$, $\sigma_{zz} = \frac{\sum_{i=1}^N (x_i - \mu_z)^2}{N}$.

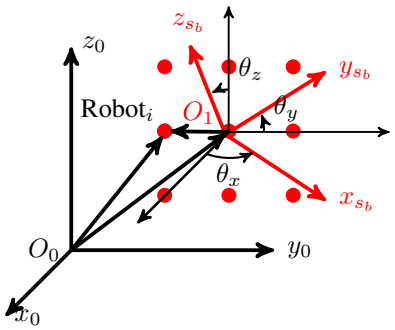

Fig. 1: Reference frames for swarm where red circles symbolically represent the UAVs; x_0, y_0, and z_0 are the basis vectors of the world frame, and x_{sb}, y_{sb}, and z_{sb} are the basis vectors of a moving frame fixed at the center of the swarm.

The covariance of the swarm distribution in a moving frame $(O_1 - x_{s_b} y_{s_b} z_{s_b})$ is given by

$$\Sigma_1 = \begin{bmatrix} s_1 & 0 & 0 \\ 0 & s_2 & 0 \\ 0 & 0 & s_3 \end{bmatrix}, \quad (11)$$

where $s_1 = \frac{1}{N} \sum_{i=1}^N p_{x_i}^2$, $s_2 = \frac{1}{N} \sum_{i=1}^N p_{y_i}^2$, $s_3 = \frac{1}{N} \sum_{i=1}^N p_{z_i}^2$, $[p_{x_i}, p_{y_i}, p_{z_i}]^{\mathrm{T}} = R_1^{0\mathrm{T}}([x_i, y_i, z_i]^{\mathrm{T}} - \mu)$, and R_1^0 is the rotation matrix describing rotations from frame $(O_0 - x_0 y_0 z_0)$ to frame $(O_1 - x_{s_b} y_{s_b} z_{s_b})$. To determine the swarm rotation angles – θ_x (rotation angle about x_0 axis), θ_y (rotation angle about y_0 axis), and θ_z (rotation angle about z_0 axis)– we relate covariance matrix Σ_0 to the covariance matrix Σ_1 as

$$\Sigma_1 = R_1^{0\mathrm{T}} \Sigma_0 R_1^0 = \begin{bmatrix} s_1 & s_{12} & s_{13} \\ s_{12} & s_2 & s_{23} \\ s_{13} & s_{23} & s_3 \end{bmatrix}, \quad (12)$$

where $s_1 = \sigma_{xx}, s_2 = \sigma_{yy}, s_3 = \sigma_{zz}$, $s_{12} = \sigma_{xy}(\cos^2\theta_x - \sin^2\theta_x) + (\sigma_{xx} - \sigma_{yy})\cos\theta_x \sin\theta_x$, $s_{13} = \sigma_{xz}(\cos^2\theta_z - \sin^2\theta_z) + (\sigma_{zz} - \sigma_{xx})\cos\theta_z \sin\theta_z$, and $s_{23} = \sigma_{yz}(\cos^2\theta_y - \sin^2\theta_y) + (\sigma_{yy} - \sigma_{zz})\cos\theta_y \sin\theta_y$. Then, from (11) and (12), the swarm rotation angles are computed as

$$\begin{aligned} \theta_x &= \frac{1}{2} tan^{-1}\left(\frac{2\sigma_{xy}}{\sigma_{yy} - \sigma_{xx}}\right) \\ \theta_y &= \frac{1}{2} tan^{-1}\left(\frac{2\sigma_{yz}}{\sigma_{zz} - \sigma_{yy}}\right) \\ \theta_z &= \frac{1}{2} tan^{-1}\left(\frac{2\sigma_{xz}}{\sigma_{xx} - \sigma_{zz}}\right). \end{aligned} \quad (13)$$

Now, let $a = \begin{bmatrix} \mu_x & \mu_y & \mu_z & \theta_x & \theta_y & \theta_z & s_1 & s_2 & s_3 \end{bmatrix}^{\mathrm{T}} \in \mathbb{R}^9$ be a vector of swarm descriptors. Also, let a surjective submersion

$$\Phi : \mathbb{R}^{3N} \to \mathbb{R}^9, \quad \Phi(x_s) = a, \quad (14)$$

relate the swarm descriptors a and the swarm configuration x_s. Then, for $i = \{1, \cdots, N\}$, using (8) and (14), we define

a new system as

$$\begin{aligned}\begin{bmatrix}\ddot{x}_i\\ \ddot{y}_i\\ \ddot{z}_i\end{bmatrix} &= \begin{bmatrix}0\\0\\g\end{bmatrix} + R_i^{\mathrm{T}}\begin{bmatrix}0\\0\\-\frac{T_i}{m}\end{bmatrix},\\ \begin{bmatrix}\dot{p}_i\\ \dot{q}_i\\ \dot{r}_i\end{bmatrix} &= \begin{bmatrix}q_i r_i \frac{I_{yy}-I_{zz}}{I_{xx}}\\ p_i r_i \frac{I_{zz}-I_{xx}}{I_{yy}}\\ p_i q_i \frac{I_{xx}-I_{yy}}{I_{zz}}\end{bmatrix} + \begin{bmatrix}\frac{1}{I_{xx}} & 0 & 0\\ 0 & \frac{1}{I_{yy}} & 0\\ 0 & 0 & \frac{1}{I_{zz}}\end{bmatrix}\begin{bmatrix}l_i\\ m_i\\ n_i\end{bmatrix},\\ y &= a.\end{aligned} \tag{15}$$

Our aim is to design a distributed control law $u_i = [T_i, l_i, m_i, n_i]^{\mathrm{T}}$ for each Quadcopter i in such a way that the motion of distribution of the swarm follows the desired trajectory $a_d = [\mu_{d_x}, \mu_{d_y}, \mu_{d_z}, \theta_{d_{sr}}, \theta_{d_{sp}}, \theta_{d_{sy}}, s_{d_l}, s_{d_w}, s_{d_h}]^{\mathrm{T}} \in \mathbb{R}^9$. However, synthesizing control law u_i necessitates each Quadcopter i to know the position information of all robots in the swarm to determine the vector of the swarm descriptors at each time t. A central observer that moves with the swarm could collect the position information of all robots in the swarm, compute the values of the swarm descriptors, and broadcast the computed values to all robots in the swarm. However, such a centralized approach is prone to high bandwidth requirements and the centralized observer can be a single point of failure. We evade these drawbacks by designing a dynamic average consensus estimator for each Quadcopter i to estimate the swarm descriptors a based on the position information collected from the neighbor robots, subsequently realizing a distributed control architecture.

Mathematically, we state the problem of collective navigation of swarm of quadcopters as follows:

Problem 1. *Consider a swarm of quadcopters Q_i, $i = \{1, \cdots, N\}$ whose motion dynamics are given in (15). Given the desired trajectory $a_d = [\mu_{d_x}, \mu_{d_y}, \mu_{d_z}, \theta_{d_{sr}}, \theta_{d_{sp}}, \theta_{d_{sy}}, s_{d_l}, s_{d_w}, s_{d_h}]^{\mathrm{T}} \in \mathbb{R}^9$ for collective motion of a quadcopter swarm,*

a) Design distributed consensus-based estimators to estimate the swarm descriptors $a = [\mu_x, \mu_y, \mu_z, \theta_{d_x}, \theta_{d_y}, \theta_{d_z}, s_l, s_w, s_h]^{\mathrm{T}}$ at time t, while handling robot drop-outs and communication link failures,

b) Design a distributed control laws u_i for each Quadcopter i, $i \in \{1, \cdots, N\}$, so that the collective motion of the swarm tracks the desired trajectory a_d.

III. Consensus-Based Distributed collective motion framework

In this section, we present the developed consensus-based distributed collective motion framework. As shown in Fig. 3, our proposed framework has the following components: the Motion planner, the UAV swarm descriptors estimator, the UAV cooperative motion controller, the UAV attitude controller, and the UAV state estimator. The Motion planner provides the desired collective motion trajectory $a_d = [\mu_{d_x}, \mu_{d_y}, \mu_{d_z}, \theta_{d_{sr}}, \theta_{d_{sp}}, \theta_{d_{sy}}, s_{d_l}, s_{d_w}, s_{d_h}]^{\mathrm{T}}$. The UAV swarm descriptors estimator is responsible to provide the estimate of the swarm descriptors $a = [\mu_x, \mu_y, \mu_z, \theta_{d_x}, \theta_{d_y}, \theta_{d_z}, s_l, s_w, s_h]^{\mathrm{T}}$ at time t. The UAV swarm descriptors estimator is built on the top of the UAV state estimator which provides the estimate of the quadcopter state $[x_i, y_i, z_i, \phi_i, \theta_i, \psi_i, u_i, v_i, w_i, p_i, q_i, r_i]^{\mathrm{T}}$. For the UAV state estimator, any common method in the literature such as Kalman Filtering can be employed. Then, this information will be used by the UAV swarm descriptors estimator to estimate swarm descriptors. Then, we design a distributed hierarchical control law for each robot so that the swarm robots can collectively follow a desired trajectory.

A. Consensus-based swarm descriptors estimator

In general, computing the vector of swarm descriptors a requires all−to−one communication (between the UAVs and a centralized observer) or all−to−all communication among the UAVs in the swarm. Such a centralized communication architecture is prone to failures associated with the centralized observer, with the UAVs in the swarm, with communication links between the observer and individual UAVs, or with communication links between the UAVs. To tackle this, we devise a more robust technique based on a distributed communication architecture to estimate the vector of swarm descriptors a. To this end, we re-write the swarm descriptors as follows:

$$a = \begin{bmatrix}\mu_x\\ \mu_y\\ \mu_z\\ \theta_x\\ \theta_y\\ \theta_z\\ s_1\\ s_2\\ s_3\end{bmatrix} = \begin{bmatrix}\frac{1}{N}\sum_{i=1}^{N}\zeta_{i_1}\\ \frac{1}{N}\sum_{i=1}^{N}\zeta_{i_2}\\ \frac{1}{N}\sum_{i=1}^{N}\zeta_{i_3}\\ \frac{1}{2}\tan^{-1}\left(\frac{\frac{\sum_{i=1}^{N}\zeta_{i_4}}{N}}{\frac{\sum_{i=1}^{N}\zeta_{i_5}}{N}}\right)\\ \frac{1}{2}\tan^{-1}\left(\frac{\frac{\sum_{i=1}^{N}\zeta_{i_6}}{N}}{\frac{\sum_{i=1}^{N}\zeta_{i_7}}{N}}\right)\\ \frac{1}{2}\tan^{-1}\left(\frac{\frac{\sum_{i=1}^{N}\zeta_{i_8}}{N}}{\frac{\sum_{i=1}^{N}\zeta_{i_9}}{N}}\right)\\ \frac{1}{N}\sum_{i=1}^{N}\zeta_{i_{10}}\\ \frac{1}{N}\sum_{i=1}^{N}\zeta_{i_{11}}\\ \frac{1}{N}\sum_{i=1}^{N}\zeta_{i_{12}}\end{bmatrix}, \tag{16}$$

where

$$\zeta_i = \begin{bmatrix}\zeta_{i_1}\\ \zeta_{i_2}\\ \zeta_{i_3}\\ \zeta_{i_4}\\ \zeta_{i_5}\\ \zeta_{i_6}\\ \zeta_{i_7}\\ \zeta_{i_8}\\ \zeta_{i_9}\\ \zeta_{i_{10}}\\ \zeta_{i_{11}}\\ \zeta_{i_{12}}\end{bmatrix} = \begin{bmatrix}x_i\\ y_i\\ z_i\\ 2(x_i-\mu_x)(y_i-\mu_y)\\ (y_i-\mu_y)^2-(x_i-\mu_x)^2\\ 2(y_i-\mu_y)(z_i-\mu_z)\\ (z_i-\mu_z)^2-(y_i-\mu_y)^2\\ 2(x_i-\mu_x)(z_i-\mu_z)\\ (x_i-\mu_x)^2-(z_i-\mu_z)^2\\ x_i^2\\ y_i^2\\ z_i^2\end{bmatrix}. \tag{17}$$

Then, to estimate $\frac{1}{N}\sum_{i=1}^{N}\zeta_{i_k}$ in a distributed way, we propose an edge-based dynamic average consensus of the form:

$$\begin{aligned}\dot{\eta}_{ij_k} &= -\rho\tanh\{c(\gamma_{i_k}-\gamma_{j_k})\}, j \in \mathcal{N}_i,\\ \gamma_{i_k} &= 2\sum_{j\in\mathcal{N}_i}\eta_{ij_k} + \zeta_{i_k},\end{aligned} \tag{18}$$

where $k = 1, \cdots, 12$, $c \geq 1$ and $\rho \in \mathbb{R}$ are global estimator parameters, η_{ij_k} is the internal state of the estimator on

This article has been accepted for publication in IEEE Internet of Things Journal. This is the author's version which has not been fully edited and content may change prior to final publication. Citation information: DOI 10.1109/JIOT.2023.3305610

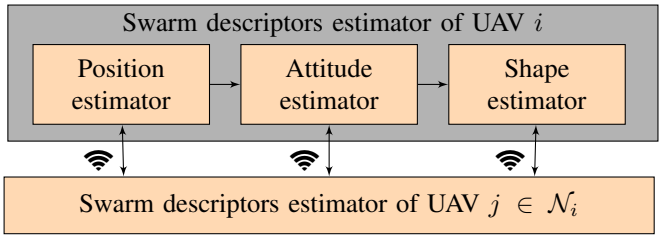

Fig. 2: Swarm descriptors estimator of UAV i.

UAV, and $\gamma_{i_k} \in \mathbb{R}$ is the estimation of $\frac{1}{N}\sum_{i=1}^{N}\zeta_{i_k}$. For a connected communication graph $\mathcal{G}(t)$, the consensus protocol in (18) is robust to UAVs joining or leaving the swarm, and communication link failures among adjacent UAVs (See Section IV-A for the proof). Further, the protocol proposed in (18) does not suffer from chattering phenomena unlike the work in [40], [42].

The swarm descriptors estimator on UAV i has three components: the position estimator, the attitude estimator, and the shape estimator. The block diagram showing the components of the swarm descriptors estimator on UAV i is portrayed in Fig. 2. Using the consensus protocol in (18), the *Position estimator* block estimates μ_x, μ_y, and μ_z as γ_{i_1}, γ_{i_2}, and γ_{i_3}, respectively. Also, the *Attitude estimator* block estimates θ_x, θ_y, and θ_z as $\frac{1}{2}\tan^{-1}\left(\frac{\gamma_{i_4}}{\gamma_{i_5}}\right)$, $\frac{1}{2}\tan^{-1}\left(\frac{\gamma_{i_6}}{\gamma_{i_7}}\right)$, and $\frac{1}{2}\tan^{-1}\left(\frac{\gamma_{i_8}}{\gamma_{i_9}}\right)$, respectively. Further, the *Shape estimator* block estimates s_1, s_2, and s_3 as $\gamma_{i_{10}}$, $\gamma_{i_{11}}$, and $\gamma_{i_{12}}$, respectively. Putting all together, the estimate of the swarm descriptors $\bar{a}$ at UAV i will be

$$\bar{a} = \begin{bmatrix} \bar{\mu}_x \\ \bar{\mu}_y \\ \bar{\mu}_z \\ \bar{\theta}_x \\ \bar{\theta}_y \\ \bar{\theta}_z \\ \bar{s}_1 \\ \bar{s}_2 \\ \bar{s}_3 \end{bmatrix} = \begin{bmatrix} \gamma_{i_1} \\ \gamma_{i_2} \\ \gamma_{i_3} \\ \frac{1}{2}\tan^{-1}\left(\frac{\gamma_{i_4}}{\gamma_{i_5}}\right) \\ \frac{1}{2}\tan^{-1}\left(\frac{\gamma_{i_6}}{\gamma_{i_7}}\right) \\ \frac{1}{2}\tan^{-1}\left(\frac{\gamma_{i_8}}{\gamma_{i_9}}\right) \\ \gamma_{i_{10}} \\ \gamma_{i_{11}} \\ \gamma_{i_{12}} \end{bmatrix}. \tag{19}$$

B. Hierarchical distributed Controller

The controller design for highly non-linear and strongly coupled swarm system in (15) is very challenging. Besides, the inherent under-actuated property of the quadcopter dynamics makes controlling all the six states of the quadcopters very difficult, while collectively moving the UAVs along the desired swarm trajectory. In this section, we develop a distributed controller to track the desired trajectory of the swarm descriptors a_d by exploiting the structural property of the quadcopters' dynamics. For this purpose, we transform the attitude dynamics to a form that is suitable for control design. We start by relating the body rates and the euler angle rates as

$$\begin{bmatrix} \dot{\phi}_i \\ \dot{\theta}_i \\ \dot{\psi}_i \end{bmatrix} = \begin{bmatrix} 1 & \frac{\sin\phi_i \sin\theta_i}{\cos\theta_i} & \frac{\cos\phi_i \sin\theta_i}{\cos\theta_i} \\ 0 & \cos\phi_i & -\sin\phi_i \\ 0 & \frac{\sin\phi_i}{\cos\theta_i} & \frac{\cos\phi_i}{\cos\theta_i} \end{bmatrix} \begin{bmatrix} p_i \\ q_i \\ r_i \end{bmatrix} \tag{20}$$

By differentiating (20) with respect to time and recalling (6), assuming small angle motions, the transformed attitude dynamics will be

$$\begin{bmatrix} \ddot{\phi}_i \\ \ddot{\theta}_i \\ \ddot{\psi}_i \end{bmatrix} = \begin{bmatrix} \dot{\theta}_i\dot{\psi}_i\frac{I_{yy}-I_{zz}}{I_{xx}} \\ \dot{\phi}_i\dot{\psi}_i\frac{I_{zz}-I_{xx}}{I_{yy}} \\ \dot{\phi}_i\dot{\theta}_i\frac{I_{xx}-I_{yy}}{I_{zz}} \end{bmatrix} + \begin{bmatrix} \frac{1}{I_{xx}} & 0 & 0 \\ 0 & \frac{1}{I_{yy}} & 0 \\ 0 & 0 & \frac{1}{I_{zz}} \end{bmatrix} \begin{bmatrix} l_i \\ m_i \\ n_i \end{bmatrix}. \tag{21}$$

Then, we re-write the quadcopter dynamics in (15) as

$$\begin{aligned} \begin{bmatrix} \ddot{x}_i \\ \ddot{y}_i \\ \ddot{z}_i \end{bmatrix} &= \begin{bmatrix} 0 \\ 0 \\ g \end{bmatrix} + R_i^{\mathrm{T}} \begin{bmatrix} 0 \\ 0 \\ -\frac{T_i}{m} \end{bmatrix}, \\ \begin{bmatrix} \ddot{\phi}_i \\ \ddot{\theta}_i \\ \ddot{\psi}_i \end{bmatrix} &= \begin{bmatrix} \dot{\theta}_i\dot{\psi}_i\frac{I_{yy}-I_{zz}}{I_{xx}} \\ \dot{\phi}_i\dot{\psi}_i\frac{I_{zz}-I_{xx}}{I_{yy}} \\ \dot{\phi}_i\dot{\theta}_i\frac{I_{xx}-I_{yy}}{I_{zz}} \end{bmatrix} + \begin{bmatrix} \frac{1}{I_{xx}} & 0 & 0 \\ 0 & \frac{1}{I_{yy}} & 0 \\ 0 & 0 & \frac{1}{I_{zz}} \end{bmatrix} \begin{bmatrix} l_i \\ m_i \\ n_i \end{bmatrix}, \\ y &= a. \end{aligned} \tag{22}$$

The quadcopter dynamics in (22) can be considered as cascade of translation and rotation subsystems coupled through a rotation matrix. Moreover, the quadcopter translation is due to attitude changes and it is affected by the changes of angles through the rotation matrix. Further, the attitude dynamics does not depend on the translation component of the model in (22). Based on this property of quadcopter dynamics, we design the hierarchical controller by decoupling the translational and attitude dynamics in (22) into two subsystems. Hence, the overall control system will have a hierarchical and distributed structure (see Figure 3) comprised of the UAV attitude control and the cooperative collective motion control loops, respectively. The cooperative collective motion controller is mainly responsible to track the desired swarm descriptors a_d. It operates on the translational dynamics of the UAV and generates the thrust command and desired attitudes for the UAV attitude controller. The UAV attitude controller is mainly responsible to stabilize the UAV rotational dynamics to the desired attitude.

Remark 1. *Similar to approaches in [43], [44], to simplify the control design approach, we decouple the framework components and ignore the interconnection terms between them. However, we will consider the interconnection between the components when providing the stability analysis of the swarm control framework.*

Cooperative Motion Controller: Now, let a virtual control v be defined as

$$v = [v_1, \cdots, v_N]^{\mathrm{T}}, \tag{23}$$

where

$$v_i = \begin{bmatrix} \ddot{x}_i \\ \ddot{y}_i \\ \ddot{z}_i \end{bmatrix} = \begin{bmatrix} 0 \\ 0 \\ g \end{bmatrix} + R_i^{\mathrm{T}} \begin{bmatrix} 0 \\ 0 \\ -\frac{T_i}{m} \end{bmatrix}. \tag{24}$$

Now, we represent the subsystem relating the collective motion of the swarm to the translational motion of the UAVs as follows:

$$\ddot{x}_s = v, \quad y = a, \tag{25}$$

where $x_s = [x_1, y_1, z_1, \cdots, x_N, y_N, z_N]^{\mathrm{T}}$. The system in (25)

This article has been accepted for publication in IEEE Internet of Things Journal. This is the author's version which has not been fully edited and content may change prior to final publication. Citation information: DOI 10.1109/JIOT.2023.3305610

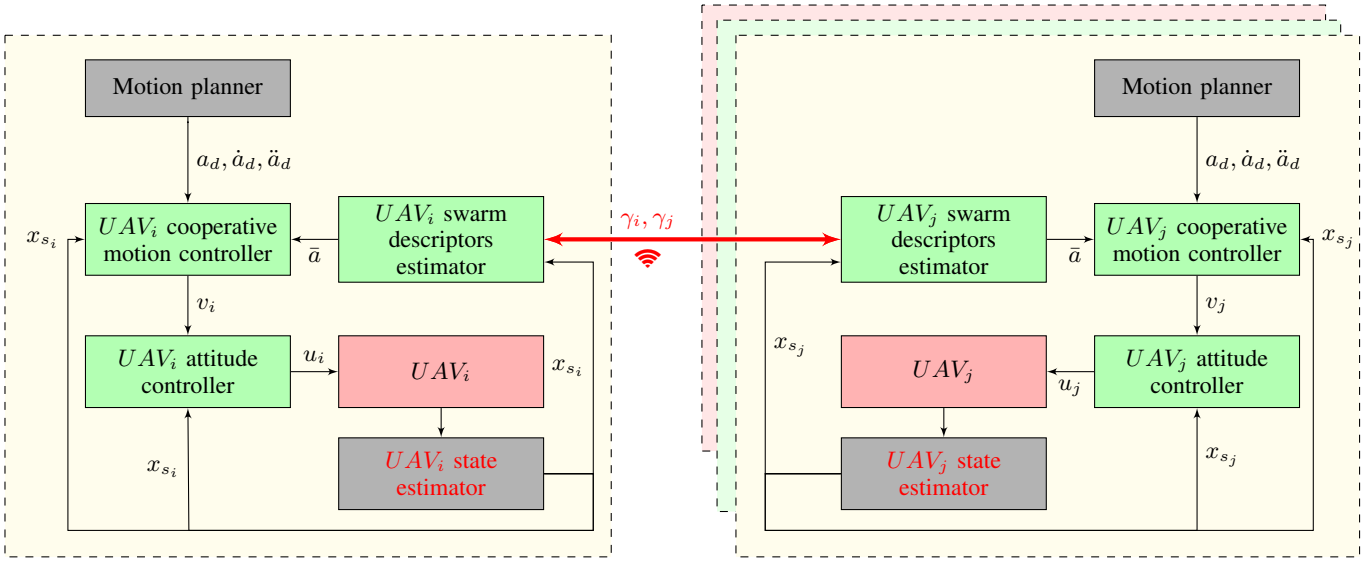

Fig. 3: A consensus-based distributed hierarchical control system architecture for UAV_i and its neighbor agents, UAV_j, $j = 1, \cdots, \mathcal{N}_i$, $j \neq i$, communicating over wireless network.

is a non-square MIMO system with $3N$ states, $3N$ inputs, and nine outputs, where the input-output relationship is non-linear. To design the virtual control v, we linearize the input-output behavior of (25) to get a linear system of the following form:

$$\ddot{a} = w, \quad y = a, \tag{26}$$

where w is the new input that steers the swarm descriptors to track the desired trajectory a_d. Since the relative degree of the system in (26) is two, we design the input w that stabilizes the following second order error dynamics

$$\ddot{e}_a + k_d \dot{e}_a + k_p e_a = 0, \tag{27}$$

where $k_d = \text{diag}(k_{d_1}, k_{d_2}, k_{d_3}, k_{d_4}, k_{d_5}, k_{d_6}, k_{d_7}, k_{d_8}, k_{d_9})$ and $k_p = \text{diag}(k_{p_1}, k_{p_2}, k_{p_3}, k_{p_4}, k_{p_5}, k_{p_6}, k_{p_7}, k_{p_8}, k_{p_9})$ are control gains, and e_a is the tracking error defined as

$$e_a = a - a_d, \tag{28}$$

where a is the current state of the swarm descriptors, and a_d is the desired trajectory of swarm descriptors. From (27), the input w can be computed as

$$w = \ddot{a}_d + k_d \dot{e}_a + k_p e_a. \tag{29}$$

Here, we use the swarm descriptors estimator (19) to compute the value of the swarm descriptors a cooperatively. Then, from input-output linearization, we relate inputs w and v as

$$v = \beta^{\#}(w - \dot{\beta}\dot{x}_s - \alpha) \tag{30}$$

where $(.)^{\#}$ is the pseudo inverse operator. Here, α and β are given as

$$\alpha = \begin{bmatrix} L_f^{r_{i1}} a_1 & \cdots & L_f^{r_{i9}} a_9 \end{bmatrix}^{\mathrm{T}}$$
$$\beta = \begin{bmatrix} L_{g_1} L_f^{r_{i1}-1} a_1 & \cdots & L_{g_{3N}} L_f^{r_{i1}-1} a_1 \\ \vdots & \ddots & \vdots \\ L_{g_1} L_f^{r_{i9}-1} a_9 & \cdots & L_{g_{3N}} L_f^{r_{i9}-1} a_9 \end{bmatrix}, \tag{31}$$

where $[a_1 \cdots a_9]^{\mathrm{T}} = \Phi(x_s)$, $r_{ij} \in N$, $i = 1, \cdots, 3N$, $j = 1, \cdots, 9$, is the relative degree for output a_j, $f = 0_{3N \times 3N}$, and $g = I_{3N \times 3N}$. $L_{f_i} a_j$ is the Lie derivative of function a_j along a vector field f_i, and $L_{g_k} L_{f_i} a_j$ is the Lie derivative of function a_j along a vector field f_i and along another vector field g_k, where $k = 1, \cdots, 3N$. Since $f = 0_{3N \times 3N}$, we have $\alpha = 0$. We also assume that $\dot{\beta}\dot{x}_s \approx 0$. The term β is computed as

$$\beta = \frac{1}{N-1} \begin{bmatrix} \frac{(x_{s_1}-\mu)^{\mathrm{T}} T_3^2}{s_2 - s_3} & \cdots & \frac{(x_{s_N}-\mu)^{\mathrm{T}} T_3^2}{s_2 - s_3} \\ \frac{(x_{s_1}-\mu)^{\mathrm{T}} T_3^1}{s_3 - s_1} & \cdots & \frac{(x_{s_N}-\mu)^{\mathrm{T}} T_3^1}{s_3 - s_1} \\ \frac{(x_{s_1}-\mu)^{\mathrm{T}} T_2^1}{s_1 - s_2} & \cdots & \frac{(x_{s_N}-\mu)^{\mathrm{T}} T_2^1}{s_1 - s_2} \\ \frac{(N-1) I_{3\times 3}}{N} & \cdots & \frac{(N-1) I_{3\times 3}}{N} \\ 2(x_{s_1}-\mu)^{\mathrm{T}} H_1 & \cdots & 2(x_{s_N}-\mu)^{\mathrm{T}} H_1 \\ 2(x_{s_1}-\mu)^{\mathrm{T}} H_2 & \cdots & 2(x_{s_N}-\mu)^{\mathrm{T}} H_2 \\ 2(x_{s_1}-\mu)^{\mathrm{T}} H_3 & \cdots & 2(x_{s_N}-\mu)^{\mathrm{T}} H_3 \end{bmatrix} \tag{32}$$

where $H_i^j = R_1^0 e_i e_j^{\mathrm{T}} (R_1^0)^{\mathrm{T}}$, $\begin{bmatrix} e_1 & e_2 & e_3 \end{bmatrix} = I_{3\times 3}$, $T_i^j = H_i^j + H_i^j$, $H_i = H_i^i$, $i, j = \{1, 2, 3\}$. Then, we compute $\beta^{\#} =$

$$\begin{bmatrix} \frac{(s_2-s_3)}{(s_2+s_3)}(x_{s_1}-\mu)^{\mathrm{T}}(T_3^2)^{\mathrm{T}} & \cdots & \frac{(s_2-s_3)}{(s_2+s_3)}(x_{s_N}-\mu)^{\mathrm{T}}(T_3^2)^{\mathrm{T}} \\ \frac{(s_3-s_1)}{(s_3+s_1)}(x_{s_1}-\mu)^{\mathrm{T}}(T_3^1)^{\mathrm{T}} & \cdots & \frac{(s_3-s_1)}{(s_3+s_1)}(x_{s_N}-\mu)^{\mathrm{T}}(T_3^1)^{\mathrm{T}} \\ \frac{(s_1-s_2)}{(s_1+s_2)}(x_{s_1}-\mu)^{\mathrm{T}}(T_2^1)^{\mathrm{T}} & \cdots & \frac{(s_1-s_2)}{(s_1+s_2)}(x_{s_N}-\mu)^{\mathrm{T}}(T_2^1)^{\mathrm{T}} \\ e_1^{\mathrm{T}} & \cdots & e_1^{\mathrm{T}} \\ e_2^{\mathrm{T}} & \cdots & e_2^{\mathrm{T}} \\ e_3^{\mathrm{T}} & \cdots & e_3^{\mathrm{T}} \\ \frac{1}{2s_1}(x_{s_1}-\mu)^{\mathrm{T}} H_1^{\mathrm{T}} & \cdots & \frac{1}{2s_1}(x_{s_N}-\mu)^{\mathrm{T}} H_1^{\mathrm{T}} \\ \frac{1}{2s_2}(x_{s_1}-\mu)^{\mathrm{T}} H_2^{\mathrm{T}} & \cdots & \frac{1}{2s_2}(x_{s_N}-\mu)^{\mathrm{T}} H_2^{\mathrm{T}} \\ \frac{1}{2s_3}(x_{s_1}-\mu)^{\mathrm{T}} H_3^{\mathrm{T}} & \cdots & \frac{1}{2s_3}(x_{s_N}-\mu)^{\mathrm{T}} H_3^{\mathrm{T}} \end{bmatrix}^{\mathrm{T}}. \tag{33}$$

Now, recalling (24), the components of the virtual input v_i

are given by

$$\begin{aligned} v_{i_x} &= -\frac{1}{m}T_i(\cos\phi_{i_d}\sin\theta_{i_d}\cos\psi_{i_d}+\sin\phi_{i_d}\sin\psi_{i_d}) \\ v_{i_y} &= -\frac{1}{m}T_i\cos\phi_{i_d}\sin\theta_{i_d}\sin\psi_{i_d}-\sin\phi_{i_d}\cos\psi_{i_d} \\ v_{i_z} &= -\frac{1}{m}T_i(\cos\phi_{i_d}\cos\theta_{i_d}+g), \end{aligned} \tag{34}$$

where v_{i_x}, v_{i_y} , and v_{i_z} are the virtual inputs along x_0, y_0, and z_0 axes, respectively, that are needed for tracking the desired trajectory a_d. We use v_x, v_y , and v_z to compute the desired trust force and desired attitude angles as

$$\begin{aligned} T_i &= m\sqrt{v_{i_x}^2+v_{i_y}^2+(g-v_{i_z})^2} \\ \phi_{i_d} &= \sin^{-1}(-m\frac{v_{i_x}\sin\psi_{i_d}-v_{i_y}\cos\psi_{i_d}}{T_i}) \\ \theta_{i_d} &= \sin^{-1}(-\frac{v_{i_x}\cos\psi_{i_d}+v_{i_y}\sin\psi_{i_d}}{g-v_{i_z}}), \end{aligned} \tag{35}$$

where $\psi_{i_d}=\theta_{z_d}$.

Remark 2. *In the autonomous mode, all the UAVs in the swarm will only be given the same swarm descriptors' reference trajectory a_d by the operator or computed by the motion planner. The attitude angles ϕ_{i_d} and θ_{i_d} and their derivatives are computed by the cooperative motion controller.*

Attitude Controller: To synthesize the required rolling, pitching, and yawing moments, we consider the attitude dynamics in (22) which is a fully-actuated system for $\theta_i \neq k\frac{\pi}{2}$. Hence, we can employ exact feedback linearization to obtain a 3D double integrator system of the form:

$$\begin{bmatrix}\ddot{\phi}_i\\ \ddot{\theta}_i\\ \ddot{\psi}_i\end{bmatrix} = \begin{bmatrix}\bar{\tau}_{\phi_i}\\ \bar{\tau}_{\theta_i}\\ \bar{\tau}_{\psi_i}\end{bmatrix}. \tag{36}$$

We design the following PD controller to stabilize the double integrator system in (36)

$$\begin{bmatrix}\bar{\tau}_{\phi_i}\\ \bar{\tau}_{\theta_i}\\ \bar{\tau}_{\psi_i}\end{bmatrix} = \begin{bmatrix}\ddot{\phi}_{i_d}\\ \ddot{\theta}_{i_d}\\ \ddot{\psi}_{i_d}\end{bmatrix} + k_{ad}\begin{bmatrix}\dot{\phi}_{i_d}-\dot{\phi}_i\\ \dot{\theta}_{i_d}-\dot{\theta}_i\\ \dot{\psi}_{i_d}-\dot{\psi}_i\end{bmatrix} + k_{ap}\begin{bmatrix}\phi_{i_d}-\phi_i\\ \theta_{i_d}-\theta_i\\ \psi_{i_d}-\psi_i\end{bmatrix}, \tag{37}$$

where k_{ad} = $\mathrm{diag}(k_{ad_1}, k_{ad_2}, k_{ad_3})$ and k_{ap} = $\mathrm{diag}(k_{ap_1}$, $k_{ap_2}, k_{ap_3})$ are control gains. Then, the body angular accelerations are obtained as

$$\begin{bmatrix}\dot{p}\\ \dot{q}\\ \dot{r}\end{bmatrix} = \begin{bmatrix}1 & 0 & -\sin\theta_i\\ 0 & \cos\phi_i & \sin\phi_i\cos\theta_i\\ 0 & -\sin\phi_i & \cos\phi_i\cos\phi_i\end{bmatrix}\begin{bmatrix}\bar{\tau}_{\phi_i}\\ \bar{\tau}_{\theta_i}\\ \bar{\tau}_{\psi_i}\end{bmatrix} + \begin{bmatrix}0\\0\\0\end{bmatrix} \\ \begin{bmatrix}0 & \cos\theta_i\dot{\theta}_i\\ \sin\phi_i\dot{\phi}_i & -\sin\phi_i\sin\theta_i\dot{\theta}_i-\cos\phi_i\cos\theta_i\dot{\phi}_i\\ \cos\phi_i\dot{\phi}_i & -\sin\theta_i\cos\phi_i\dot{\theta}_i+\sin\phi_i\cos\theta_i\dot{\phi}_i\end{bmatrix}\begin{bmatrix}\dot{\phi}_i\\ \dot{\theta}_i\\ \dot{\psi}_i\end{bmatrix}. \tag{38}$$

From the body angular accelerations computed in (38), we compute the required rolling, pitching, and yawing moments as

$$\begin{bmatrix}l_i\\ m_i\\ n_i\end{bmatrix} = \begin{bmatrix}I_{xx}\dot{p}_i+(I_{zz}-I_{yy})qr\\ I_{yy}\dot{q}_i+(I_{xx}-I_{zz})pr\\ I_{zz}\dot{r}_i+(I_{yy}-I_{xx})pq\end{bmatrix}. \tag{39}$$

IV. Stability and convergence analysis

In this section, recalling that the proposed control framework for swarm of quadcopters has three interconnected subsystems, i.e., the consensus based swarm descriptors estimator, the cooperative motion controller, and the attitude controller subsystems, we analyze the stability of each the subsystems followed by the stability analysis of the overall system.

To begin, let the estimate of the swarm descriptors $\bar{a} = (a+\delta a)$, where δa is the estimation error. Also, assume δa is slowly varying, i.e, $\delta\dot{a}\approx 0$. We can then rewrite (29) as

$$w_{new} = \ddot{a}_d + k_d(\dot{a}-\dot{a}_d) + k_p(a-a_d) + k_p\delta a. \tag{40}$$

Then, the new virtual control input v_{new} can be written as

$$v_{new} = \beta_{new}^{\#} w_{new}, \tag{41}$$

where $\beta_{new} = (\beta+\Delta\beta)$ and $\Delta\beta$ is due to δa. Assuming $\dot{\beta}_{new}=\dot{\beta}$, i.e., $\Delta\dot{\beta}=0$, and using properties of matrix ($(\beta+\Delta\beta)^{\#}=\beta^{\#}+\tilde{\beta}$, and $\tilde{\beta}=(\beta^{\mathrm{T}}\beta)^{-1}\Delta\beta-(\beta^{\mathrm{T}}\beta)^{-1}(2\beta^{\mathrm{T}}\Delta\beta+\Delta\beta^{\mathrm{T}}\Delta\beta)(\beta^{\mathrm{T}}\beta+2\beta^{\mathrm{T}}\Delta\beta+\Delta\beta^{\mathrm{T}}\Delta\beta)^{-1}(\beta^{\mathrm{T}}+\Delta\beta^{\mathrm{T}})$), we have

$$v_{new} = \beta^{\#}w + \Delta_1, \tag{42}$$

where $\Delta_1 = (\beta^{\#}+\tilde{\beta})k_p\delta a + \tilde{\beta}w$. Similarly, in (24) by replacing (ϕ_i,θ_i,ψ_i) by $(\phi_{i_d}+e_{\phi_i},\theta_{i_d}+e_{\theta_i},\psi_{i_d}+e_{\psi_i})$ where $e_{\phi_i}=\phi_{i_d}-\phi_i$, $e_{\theta_i}=\theta_{i_d}-\theta_i$, $e_{\psi_i}=\psi_{i_d}-\psi_i$, and recalling (36), the overall system on Quadcopter i will be

$$\begin{aligned} \ddot{x}_{s_i} &= v_i+\Delta_1+\Delta_2, \\ \ddot{\phi}_i &= \bar{\tau}_{\phi_i}, \\ \ddot{\theta}_i &= \bar{\tau}_{\theta_i}, \\ \ddot{\psi}_i &= \bar{\tau}_{\psi_i}, \end{aligned} \tag{43}$$

where $\Delta_2 = -\frac{1}{m}T_ih_i(\phi_{i_d},\theta_{i_d},\psi_{i_d},e_{\phi_i},e_{\theta_i},e_{\psi_i})$ and $h_i = (h_{x_i},h_{y_i},h_{z_i})$ can be computed as follows:

$$\begin{aligned} h_{x_i} &= (h_{3_i}\sin\theta_{i_d}-h_{6_i}\cos\phi_{i_d}-h_{3_i}h_{6_i})\cos\psi_{i_d}, \\ &\quad -(h_{5_i}\cos\phi_{i_d}+h_{5_i}h_{3_i})\sin\theta_{i_d}-h_{4_i}\sin\phi_{i_d} \\ &\quad +h_{1_i}\sin\psi_{i_d}-h_{6_i}h_{5_i}\cos\phi_{i_d}-h_{1_i}h_{4_i}-h_{3_i}h_{5_i}h_{6_i} \\ h_{y_i} &= (h_{3_i}\sin\theta_{i_d}-h_{6_i}\cos\phi_{i_d}-h_{3_i}h_{6_i})\sin\psi_{i_d} \\ &\quad -(h_{4_i}\cos\phi_{i_d}+h_{4_i}h_{3_i})\sin\theta_{i_d}-h_{5_i}\sin\phi_{i_d} \\ &\quad -(h_{1_i}-h_{6_i}h_{4_i})\cos\psi_{i_d}-h_{1_i}h_{5_i}-h_{3_i}h_{4_i}h_{6_i}, \\ h_{z_i} &= h_{2_i}h_{3_i}+h_{2_i}\cos\phi_{i_d}+h_{3_i}\cos\theta_{i_d} \end{aligned} \tag{44}$$

and

$$\begin{aligned} h_{1_i} &= \sin(e_{\phi_i}/2)\cos(\phi_{i_d}+e_{\phi_i}/2), \\ h_{2_i} &= -\sin(e_{\theta_i}/2)\sin(\theta_{i_d}+e_{\theta_i}/2), \\ h_{3_i} &= -\sin(e_{\phi_i}/2)\sin(\phi_{i_d}+e_{\phi_i}/2), \\ h_{4_i} &= -\sin(e_{\psi_i}/2)\cos(\psi_{i_d}+e_{\psi_i}/2), \\ h_{5_i} &= -\sin(e_{\psi_i}/2)\sin(\psi_{i_d}+e_{\psi_i}/2), \\ h_{6_i} &= -\sin(e_{\theta_i}/2)\cos(\theta_{i_d}+e_{\theta_i}/2). \end{aligned} \tag{45}$$

Remark 3. *The terms Δ_1 and Δ_2 in fact represent the interconnection between the system's components. More specifically, Δ_1 captures the interconnection between the swarm descriptors estimator and the cooperative motion controller*

This article has been accepted for publication in IEEE Internet of Things Journal. This is the author's version which has not been fully edited and content may change prior to final publication. Citation information: DOI 10.1109/JIOT.2023.3305610

and Δ_2 captures the interconnection between the cooperative motion controller and the attitude controller subsystems.

Now, using the theory on the stability of cascade systems presented in [43]–[45], we show that the interconnection terms Δ_1 and Δ_2 satisfies a growth restriction condition (see Theorem 3 from [43]), which can then be leveraged to show the stability of the overall system. Accordingly, the stability analysis process can be broken down into the following parts:

- Prove that the swarm descriptors estimator guarantees a bounded estimation error δa.
- Prove that the cooperative motion controller and the attitude controller are globally exponentially stable in the absence of the interconnection terms Δ_1 and Δ_2.
- Prove that the interconnection terms Δ_1 and Δ_2 satisfies the growth restriction condition so that the overall closed loop system is asymptotically stable.

Next, we will provide the proof for the above stated problems.

A. Convergence analysis of the swarm descriptors estimator

Consider the consensus based swarm descriptors estimators (18) of all the UAVs in the swarm, which can be put together as

$$\begin{aligned}\dot{\bar{\eta}}_k &= -\rho \tanh\{c\mathcal{B}^{\mathrm{T}}(t)\bar{\gamma}_k\}\\ \bar{\gamma}_k &= \mathcal{B}(t)\bar{\eta}_k + \bar{\zeta}_k,\end{aligned} \tag{46}$$

where $k = 1, \cdots, 12$, $\bar{\eta}_k(t) = [\eta_{1k}, \cdots, \eta_{Nk}]^{\mathrm{T}}$, $\eta_{ik} = \{\eta_{ij_k}\}_{j\in\mathcal{N}_i}$, $i = 1, \cdots, N$, $\bar{\gamma}_k(t) = [\gamma_{1k}, \cdots, \gamma_{Nk}]^{\mathrm{T}}$, $\bar{\zeta}_k(t) = [\zeta_{1k}, \cdots, \zeta_{Nk}]^{\mathrm{T}}$, $\mathcal{B}(t)$ is the incidence matrix of the swarm communication graph $\mathcal{G}(t)$, and $\tanh(.)$ is applied component wise.

Theorem 1. *Consider a swarm with a strongly connected bidirectional graph $\mathcal{G}(t)$ and time-varying $\bar{\zeta}_k$ with bounded first derivative. The proposed consensus based swarm descriptors estimators (46) guarantee that the estimation error $\tilde{\gamma}_k = |\bar{\gamma}_k - \frac{\mathbf{1}_N\mathbf{1}_N^{\mathrm{T}}}{N}\bar{\zeta}_k|$ is uniformly ultimately bounded and converges to the adjustable compact set given by*

$$\{\tilde{\gamma}_k : \|\tilde{\gamma}_k\|_\infty \leq \left\|\left(\mathcal{B}^{\mathrm{T}}(t)\right)^{+}\right\|_2 \left(\sqrt{\frac{N\lambda_{max}\left(\mathcal{L}(t)\right)}{\lambda_2\left(\mathcal{L}(t)\right)}}\right)\delta\}, \tag{47}$$

where $\lambda_2(\mathcal{L}(t))$ is the algebraic connectivity of $\mathcal{G}(t)$, $\lambda_{max}(\mathcal{L}(t))$ is the maximum eigenvalue of $\mathcal{L}(t)$, $\delta = \frac{1}{2c}\ln\left(\frac{\rho+\left\|\dot{\bar{\zeta}}_k\right\|_1}{\rho-\left\|\dot{\bar{\zeta}}_k\right\|_1}\right)$ for all $\tilde{\gamma}_k(t_0)$, $k = 1, \cdots, 12$, if and only if the global consensus parameters are selected as $\rho \gg \max_k(\sup_{t\geq t_0}\left\|\dot{\bar{\zeta}}_k\right\|_1)$ and $c \geq 1$.

Proof. From the consensus based swarm descriptors estimators in (46), the swarm descriptors estimation error and estimation error derivatives are given by

$$\begin{aligned}\tilde{\gamma}_k &= \bar{\gamma}_k - \frac{\mathbf{1}_N\mathbf{1}_N^{\mathrm{T}}}{N}\bar{\zeta}_k\\ \dot{\tilde{\gamma}}_k &= \mathcal{B}(t)\dot{\bar{\eta}}_k + M\dot{\bar{\zeta}}_k,\end{aligned} \tag{48}$$

where $M = (I_N - \frac{\mathbf{1}_N\mathbf{1}_N^{\mathrm{T}}}{N})$. Using (48), Lemmas 1 and 2, we have $\mathbf{1}_N^T\mathcal{B}(t) = 0$, $\mathcal{B}^{\mathrm{T}}(t)\mathbf{1}_N = 0$, $\mathbf{1}_N^{\mathrm{T}}\tilde{\gamma}_k = 0$, and $\mathcal{B}^{\mathrm{T}}(t)\tilde{\gamma}_k = \mathcal{B}^{\mathrm{T}}(t)\bar{\gamma}_k$. Now, consider the Lyapunov function of the form $V \triangleq \frac{1}{2}\tilde{\gamma}_k^{\mathrm{T}}\tilde{\gamma}_k$ and invariant set

$$\Omega_{d_c} = \{V \leq d_c\}, \Omega_\epsilon = \{V \leq \epsilon\}, \Lambda = \{\epsilon \leq V \leq d_c\} \tag{49}$$

for some $d_c \geq \epsilon \geq \frac{\delta^2}{2}$. Taking the derivative of V, we have

$$\dot{V} = -\vartheta_k^{\mathrm{T}}\rho\tanh(c\vartheta_k) + \vartheta_k^{\mathrm{T}}\mathcal{B}^{\mathrm{T}}(t)\left(\mathcal{B}(t)\mathcal{B}^{\mathrm{T}}(t)\right)^{+}\dot{\bar{\zeta}}_k, \tag{50}$$

where

$$\vartheta_k = \mathcal{B}^{\mathrm{T}}(t)\tilde{\gamma}_k = \mathcal{B}^{\mathrm{T}}(t)\bar{\gamma}_k. \tag{51}$$

Let $\Theta_i = m_{i1}\dot{\bar{\zeta}}_{1_k} + \cdots + m_{iN}\dot{\bar{\zeta}}_{N_k}$, where m_{ij}, $i = 1, \cdots, l$, $j = 1, \cdots, N$, are the elements of $\mathcal{B}^{\mathrm{T}}(t)\left(\mathcal{B}(t)\mathcal{B}^{\mathrm{T}}(t)\right)^{+}$, l is the total number of edges in $\mathcal{G}(t)$, and $(.)^+$ is the generalized inverse. Then, expanding $\dot{V}$, we have

$$\begin{aligned}\dot{V} = -\rho[\vartheta_{1k}\tanh(c\vartheta_{1k}) + \cdots + \vartheta_{lk}\tanh(c\vartheta_{lk})]\\ + \vartheta_{1k}\Theta_1 + \cdots + \vartheta_{lk}\Theta_l.\end{aligned} \tag{52}$$

Now, letting $w_i(\vartheta_{ik}) = -\rho\vartheta_{ik}\tanh(c\vartheta_{ik}) + \vartheta_{ik}\Theta_i$, we can re-write $\dot{V}$ as

$$\dot{V} = \sum_{i=1}^{l} w_i(\vartheta_{ik}). \tag{53}$$

Since $\tanh(\vartheta_{ik}) = \mathrm{sgn}(c\vartheta_{ik})\left(1 - \frac{2}{e^{2c|\vartheta_{ik}|}+1}\right)$, the term $w_i(\vartheta_{ik})$ will be given as

$$\begin{aligned}w_i(\vartheta_{ik}) = -\rho\vartheta_{ik}\left(\mathrm{sgn}(c\vartheta_{ik})\left(1 - \frac{2}{e^{2c|\vartheta_{ik}|}+1}\right)\right)\\ + \vartheta_{ik}\Theta_i.\end{aligned} \tag{54}$$

Then, since $\vartheta_{ik}\,\mathrm{sgn}(c\vartheta_{ik}) = |\vartheta_{ik}|$, and $|\Theta_i| \leq \sum_{i=1}^{N}|\dot{\bar{\zeta}}_{i_k}| = \left\|\dot{\bar{\zeta}}_k\right\|_1$, we have

$$\begin{aligned}w_i(\vartheta_{ik}) &= -|\vartheta_{ik}|(\rho - \frac{2\rho}{e^{2c|\vartheta_{ik}|}+1} - |\Theta_i|),\\ &\leq -|\vartheta_{ik}|\rho + |\vartheta_{ik}|\frac{2\rho}{e^{2c|\vartheta_{ik}|}+1} + |\vartheta_{ik}|\sum_{i=1}^{N}|\dot{\bar{\zeta}}_{i_k}|.\end{aligned} \tag{55}$$

We have $w_i(\vartheta_{ik}) < 0$ if and only if $|\vartheta_{ik}| > 0$ and $(\rho - \frac{2\rho}{e^{2c|\vartheta_{ik}|}+1} - \left\|\dot{\bar{\zeta}}_k\right\|_1) > 0$. Accordingly, we have $(\rho - \frac{2\rho}{e^{2c|\vartheta_{ik}|}+1} - \left\|\dot{\bar{\zeta}}_k\right\|_1) > 0$ if and only if

$$\begin{aligned}|\vartheta_{ik}| > \frac{1}{2c}\ln\left(\frac{\rho+\left\|\dot{\bar{\zeta}}_k\right\|_1}{\rho-\left\|\dot{\bar{\zeta}}_k\right\|_1}\right), \text{and}\\ \rho > \left\|\dot{\bar{\zeta}}_k\right\|_1\end{aligned} \tag{56}$$

Then, from (52-56), we can conclude that $\dot{V} = \sum_{i=1}^{l} w_i(\vartheta_{ik}) < 0$ for all $\|\vartheta_k\|_\infty > \delta$, $\rho > \left\|\dot{\bar{\zeta}}_k\right\|_1$, and $c \geq 1$, where

$$\delta = \frac{1}{2c}\ln\left(\frac{\rho+\left\|\dot{\bar{\zeta}}_k\right\|_1}{\rho-\left\|\dot{\bar{\zeta}}_k\right\|_1}\right). \tag{57}$$

This article has been accepted for publication in IEEE Internet of Things Journal. This is the author's version which has not been fully edited and content may change prior to final publication. Citation information: DOI 10.1109/JIOT.2023.3305610

Now, choosing ϵ and d_c such that $\frac{\delta^2}{2} \leq \epsilon \leq d_c$, then $\dot{V}$ is negative definite in the invariant set $\Lambda = \{\epsilon \leq V \leq d_c\}$. Besides, by employing Courant-Fischer Theorem [46], we have $\frac{\lambda_2(\mathcal{L}(t))}{N} \|\tilde{\gamma}_k\|_2^2 \leq V \leq \lambda_{max}(\mathcal{L}(t)) \|\tilde{\gamma}_k\|_2^2$, where $\lambda_2(\mathcal{L}(t))$ is the algebraic connectivity of $\mathcal{G}(t)$ and $\lambda_{max}(\mathcal{L}(t))$ is the maximum eigenvalue of $\mathcal{L}(t)$. Since V is radially unbounded, by defining $\alpha_1(r) \in \mathcal{K}_\infty$ and $\alpha_2(r) \in \mathcal{K}_\infty$ as

$$\begin{aligned} \alpha_1(r) &= \frac{\lambda_2(\mathcal{L}(t))}{N} r^2, \\ \alpha_2(r) &= \lambda_{max}(\mathcal{L}(t)) r^2. \end{aligned} \tag{58}$$

the ultimate bound for $\|\vartheta_k\|_\infty$ can be given as

$$\|\vartheta_k\|_\infty \leq \alpha_1^{-1}(\alpha_2(\delta)) = \left(\sqrt{\frac{N\lambda_{max}(\mathcal{L}(t))}{\lambda_2(\mathcal{L}(t))}}\right)\delta. \tag{59}$$

Substituting (59) in (51), the ultimate bound on the consensus error $\tilde{\gamma}_k = \left(\mathcal{B}^{\mathrm{T}}(t)\right)^+ \vartheta_k$ is given as

$$\begin{aligned} \|\tilde{\gamma}_k\|_\infty &= \left\|\left(\mathcal{B}^{\mathrm{T}}(t)\right)^+ \vartheta_k\right\| \leq \left\|\left(\mathcal{B}^{\mathrm{T}}(t)\right)^+\right\|_\infty \|\vartheta_k\|_\infty, \\ &\leq \left\|\left(\mathcal{B}^{\mathrm{T}}(t)\right)^+\right\|_2 \left(\sqrt{\frac{N\lambda_{max}(\mathcal{L}(t))}{\lambda_2(\mathcal{L}(t))}}\right)\delta. \end{aligned} \tag{60}$$

Further, from (57), by choosing $\rho \gg \max_k(\sup_{t\geq t_0} \left\|\dot{\tilde{\zeta}}_k\right\|_1)$, we have $\delta \approx 0$. Accordingly, from (60), we can conclude that the consensus error can be adjusted to $\|\tilde{\gamma}_k\|_\infty \approx 0$ by increasing the global consensus parameter ρ. □

Corollary 1. *The estimation error of the proposed swarm descriptors estimators (46) is bounded.*

Proof. Choosing $\rho \gg \max_k(\sup_{t\geq t_0} \left\|\dot{\tilde{\zeta}}_k\right\|_1)$ and using the relationship in (60), we can guarantee that the estimation error is bounded since $\left\|\left(\mathcal{B}^{\mathrm{T}}(t)\right)^+\right\|_2$, $\left(\sqrt{\frac{N\lambda_{max}(\mathcal{L}(t))}{\lambda_2(\mathcal{L}(t))}}\right)$, and δ are all bounded. Further, let

$$\begin{aligned} b = \min_{\vartheta\in\Lambda}(&-\sum_{i=1}^{l} w_i(\vartheta_{ik}), \\ \text{s.t.} \quad &\rho > \left\|\dot{\tilde{\zeta}}_k\right\|_1. \end{aligned} \tag{61}$$

Then, from (49), (51) and (52), we have $\dot{V} \leq -b < 0$, for all $\vartheta \in \Lambda$, for all $t \geq t_0 \geq 0$. Accordingly, $V \leq V(t_0) - b(t - t_0) \leq d_c - b(t - t_0)$, and hence, the estimation error enters the adjustable compact set within finite time $t^* = t_0 + \frac{d_c - \epsilon}{b}$. □

Corollary 2. *The proposed swarm descriptors estimators in (46) are robust to communication link failures and to UAVs leaving or joining the swarm as long as as the underlying swarm communication graph $\mathcal{G}(t)$ remains strongly connected.*

Proof. From Theorem 1 and Corollary 1, the estimation error converges to a bounded and adjustable steady-state error. However, the steady-state error is a function of the algebraic connectivity $\lambda(\mathcal{L}(t))$ of the underlying swarm communication graph $\mathcal{G}(t)$. If $\mathcal{G}(t)$ is not connected, the bound of the estimation error (48) will be undefined since the algebraic connectivity of $\mathcal{G}(t)$ is zero. On the contrary, If $\mathcal{G}(t)$ is connected, its algebraic connectivity is different from zero. Therefore, as long as the swarm communication graph $\mathcal{G}(t)$ remains connected after new UAVs join or member UAVs leave the swarm, our swarm descriptors estimator always converges to the desired value. Further, using the same argument, we guarantee that our swarm descriptors estimator converges to the desired value in the presence of communication link failures among the UAVs. □

Corollary 3. *For a strongly connected swarm communication graph $\mathcal{G}(t)$, the swarm descriptors estimators in (46) do not require special initialization.*

Proof. From the error dynamics in (48), we have $\mathbf{1}_N^{\mathrm{T}} \tilde{\gamma}_k(t) = 0$, $\mathbf{1}_N^{\mathrm{T}} \dot{\tilde{\gamma}}_k(t) = 0$, as $\mathbf{1}_N^{\mathrm{T}} \mathcal{B}(t) \bar{\eta}_k(t) = 0$ and $\mathbf{1}_N^{\mathrm{T}} M \bar{\zeta}_k(t) = 0$ for all $t \geq t_0$. Also, for a strongly connected graph $\mathcal{G}(t)$, we have $\mathcal{B}^{\mathrm{T}}(t)\mathbf{1}_N = 0$, for all $t \geq t_0$. Accordingly, $\bar{\eta}_k(t)$ can attain any value for all $t \geq t_0$, i.e., $\bar{\eta}_k(t)$ is not required to satisfy any constraints unlike the approach in [47] where $\mathbf{1}_N \bar{\eta}_k(t_0) = 0$ is needed. Therefore, the consensus protocol in (46) does not require any special initialization. □

Remark 4. *In practical scenarios, achieving consensus on the estimation of swarm descriptors can be challenging when one involves a large number of quadcopters in the swarm. However, in our proposed swarm control framework, swarm descriptors estimators do not require special initialization, and the swarm descriptors estimator and the control synthesis are decoupled. Based on these features, similar to the approaches employed in [48], the estimation procedures in swarm descriptors estimators can benefit from warm start and accelerated communications to propagate the estimates across the swarm so that the consensus can be reached quickly. Compared to [48], the recursive computation of gossiping step in the Multi-Step Dual Accelerated algorithm is replaced with a single computation using* $\tanh(.)$ *function which simplifies the procedure.*

B. Stability analysis of the cooperative motion controller and the attitude controller

In this section, recalling the control laws (30) and (37), we prove the global exponential stability of the cooperative motion controller and the attitude controller without considering the interconnection terms Δ_1 and Δ_2.

Proposition 1. *In the absence of interconnection terms Δ_1 and Δ_2, the closed loop system (43) is globally exponentially stable (GES).*

Proof. Ignoring Δ_1 and Δ_2 in (43), the cooperative motion controller on UAV i is given as

$$\ddot{x}_{s_i} = v_i. \tag{62}$$

Putting together the cooperative motion controllers of UAVs (62) in the swarm and recalling (30), we get

$$\begin{aligned} \ddot{x}_s &= v, \\ \ddot{x}_s &= \beta^{\#}(w - \dot{\beta}\dot{x}_s), \end{aligned} \tag{63}$$

This article has been accepted for publication in IEEE Internet of Things Journal. This is the author's version which has not been fully edited and content may change prior to final publication. Citation information: DOI 10.1109/JIOT.2023.3305610

where $\ddot{x}_s = \left[\ddot{x}_{s_1}, \cdots, \ddot{x}_{s_N}\right]^{\mathrm{T}}$ and $v = \left[v_1, \cdots, v_N\right]^{\mathrm{T}}$. Then, recalling the input-output relationship (26) and the control law (29), the cooperative motion controllers (63) can be rearranged as

$$\begin{aligned} \beta\ddot{x}_s + \dot{\beta}\dot{x}_s &= w, \\ \beta\ddot{x}_s + \dot{\beta}\dot{x}_s &= \ddot{a}. \end{aligned} \tag{64}$$

Also, from (64) and from the relationships in (26) and (29), we have

$$\begin{aligned} \ddot{a} &= w, \\ \ddot{a} &= \ddot{a}_d + k_d(\dot{a} - \dot{a}_d) + k_p(a - a_d). \end{aligned} \tag{65}$$

Then, from (65), we write the tracking error as:

$$\begin{bmatrix} \dot{e}_a \\ \ddot{e}_a \end{bmatrix} = \begin{bmatrix} 0_{9\times 9} & I_{9\times 9} \\ k_p & k_d \end{bmatrix} \begin{bmatrix} e_a \\ \dot{e}_a \end{bmatrix}. \tag{66}$$

Now, let $e_\phi = \left[e_{\phi_1}, \cdots, e_{\phi_N}\right]^{\mathrm{T}}$, $e_\theta = \left[e_{\theta_1}, \cdots, e_{\theta_N}\right]^{\mathrm{T}}$, $e_\phi = [e_{\psi_1}, \cdots, e_{\psi_N}]^{\mathrm{T}}$, $K_{ap} = \mathrm{diag}(k_{ap}, k_{ap}, k_{ap})$, $K_{ad} = \mathrm{diag}(k_{ad}, k_{ad}, k_{ad})$, and $\chi = [e_a, e_\phi, e_\theta, e_\psi, \dot{e}_a, \dot{e}_\phi, \dot{e}_\theta, \dot{e}_\psi]^{\mathrm{T}}$. Then, using (36), (37) and (66), we combine the cooperative motion controllers and attitude controllers of UAVs in the swarm as

$$\dot{\chi} = A_\chi \chi, \tag{67}$$

where

$$A_\chi = \begin{bmatrix} O_1 & O_2 & O_2 & O_2 & I_1 & O_2 & O_2 & O_2 \\ O_1 & O_2 & O_2 & O_2 & O_1 & I_2 & O_2 & O_2 \\ O_1 & O_2 & O_2 & O_2 & O_1 & O_2 & I_2 & O_2 \\ O_1 & O_2 & O_2 & O_2 & O_1 & O_2 & O_2 & I_2 \\ \bar{k}_p & O_2 & O_2 & O_2 & \bar{k}_d & O_2 & O_2 & O_2 \\ O_1 & \bar{k}_{ap} & O_2 & O_2 & O_1 & \bar{k}_{ad} & O_2 & O_2 \\ O_1 & O_2 & \bar{k}_{ap} & O_2 & O_1 & O_2 & \bar{k}_{ad} & O_2 \\ O_1 & O_2 & O_2 & \bar{k}_{ap} & O_1 & O_2 & O_2 & \bar{k}_{ad} \end{bmatrix},$$

and $O_1 = 0_{9\times 9}$, $O_2 = 0_{N\times N}$, $I_1 = I_{9\times 9}$, $I_2 = I_{N\times N}$, $\bar{k}_p = k_p I_1$, $\bar{k}_d = k_d I_1$, $\bar{k}_{ap} = k_{ap} I_2$, $\bar{k}_d = k_{ad} I_2$.

It is now straightforward to prove the global exponential stability of (67) by defining a positive definite radially unbounded function

$$V(\chi) = \frac{1}{2}\chi^{\mathrm{T}} P \chi, \tag{68}$$

where $P = P^T > 0$ Taking derivatives, we obtain

$$\dot{V} = -\chi^{\mathrm{T}} Q \chi \leq 0, \tag{69}$$

where $Q = -(A_\chi^{\mathrm{T}} P + P A_\chi) > 0$. Using the fact that $V(\chi) = \frac{1}{2}\chi^{\mathrm{T}} P \chi \leq \lambda_{max}[P] \left\|\chi\right\|^2$ and $\chi^{\mathrm{T}} Q \chi \geq \lambda_{min}[Q] \left\|\chi\right\|^2$, we conclude that

$$\dot{V} = -\chi^{\mathrm{T}} Q \chi \leq -\lambda_{min}[Q] \left\|\chi\right\|^2 \leq -\frac{\lambda_{min}[Q]}{\lambda_{min}[P]} V. \tag{70}$$

Also, since $V(\chi)$ is non-increasing function, from (69) and (70), we can conclude that (67) is GES. □

C. Stability analysis of the overall framework

In this section, we first provide conditions for boundedness of the interconnection and coupling terms Δ_1 and Δ_2 in (43). Then, we provide the overall stability of the overall system. Before proving the boundedness of Δ_1, we first show that $\beta^{\#}$ is bounded as:

Lemma 3. *For a finite swarm with bounded initial configuration, $\left\|\beta^{\#}\right\|_\infty \leq \hat{\beta} < \infty$ if*

$$\begin{aligned} 0 < & N_{\mu_1} \leq \left\|\mu - \mu_d\right\| \leq M_\mu, \\ 0 < & N_{s_1} \leq \left|s_1 - s_{d_1}\right| \leq M_{s_1}, \\ 0 < & N_{s_2} \leq \left|s_2 - s_{d_2}\right| \leq M_{s_2}, \\ 0 < & N_{s_3} \leq \left|s_3 - s_{d_3}\right| \leq M_{s_3}, \end{aligned} \tag{71}$$

where N_{μ_1}, N_{s_1}, N_{s_2}, N_{s_3}, M_μ, M_{s_1}, M_{s_2}, and M_{s_3} are positive constants.

Proof. For the swarm with bounded initial configuration with conditions (71), we have $|\frac{s_2 - s_3}{s_2 + s_3}|$, $|\frac{s_3 - s_1}{s_3 + s_1}|$, $|\frac{s_1 - s_2}{s_1 + s_2}|$, $|\frac{1}{s_1}|$, $|\frac{1}{s_2}|$, and $|\frac{1}{s_3}|$ bounded. Further, using (11), the summation of swarm shape parameters s_1, s_2, and s_3, will be

$$s_1 + s_2 + s_3 = \frac{1}{N-1}\sum_{i=1}^{N} (x_{s_i} - \mu)^T (x_{s_i} - \mu), \tag{72}$$

where $i = 1, \cdots, N$. Then, from (71), and (72), we have

$$\begin{aligned} \left\|x_{s_i} - \mu\right\|_2 &\leq \sqrt{(N-1)(s_1 + s_2 + s_3)} \\ &\leq \sqrt{(N-1)\bar{M}}, \end{aligned} \tag{73}$$

where $\bar{M} = M_{s_1} + M_{s_2} + M_{s_3} + s_{d_1} + s_{d_2} + s_{d_3}$. On the hand, from (33), we have

$$\begin{aligned} \left\|\beta^{\#}\right\|_\infty = \max_{i=1,\cdots,N} \Bigg\| \Bigg(& \frac{(s_2 - s_3)}{(s_2 + s_3)} T_3^2 (x_{s_i} - \mu) + \\ & \frac{(s_3 - s_1)}{(s_3 + s_1)} T_3^1 (x_{s_i} - \mu) + \frac{(s_1 - s_2)}{(s_1 + s_2)} T_2^1 (x_{s_i} - \mu) + \\ & e_1 + e_2 + e_3 + \frac{1}{2s_1} H_1 (x_{s_i} - \mu) + \\ & \frac{1}{2s_2} H_2 (x_{s_i} - \mu) + \frac{1}{2s_3} H_3 (x_{s_i} - \mu) \Bigg) \Bigg\|_\infty. \end{aligned} \tag{74}$$

Then, from (73) and (74), the boundedness on $\beta^{\#}$ is given as

$$\left\|\beta^{\#}\right\|_\infty \leq \hat{\beta} < \infty. \tag{75}$$

where

$$\begin{aligned} \hat{\beta} = 3 + & \\ & \sqrt{(N-1)(M_{s_1} + M_{s_2} + M_{s_3} + s_{d_1} + s_{d_2} + s_{d_3}}\Bigg(3 + \\ & \frac{1}{2(N_{s_1} + s_{d_1})} + \frac{1}{2(N_{s_2} + s_{d_2})} + \frac{1}{2(N_{s_3} + s_{d_3})} \Bigg). \end{aligned}$$

□

Corollary 4. *For a finite swarm with bounded initial configuration and $s_1 \neq 0$, $s_2 \neq 0$, and $s_3 \neq 0$, if the global consensus parameters are selected as $\rho \gg \max_k(\sup_{t\geq t_0} \left\|\dot{\bar{\zeta}}_k\right\|_1)$ and $c \geq 1$, then Δ_1 is bounded.*

Proof. From (41), we can see that the interconnection term Δ_1 is due to the estimation error δa. Assuming $\Delta\beta_{ij} \in \Delta\beta$ is a very small number, from (42), we can approximate Δ_1 as

$$\Delta_1 = \beta^{\#} k_p \delta a. \tag{76}$$

Now, using the conditions for boundedness of the estimation error δa (see Theorem 1) and $\beta^{\#}$ (see Lemma 3), we can conclude the boundedness of Δ_1. □

Similarly, we show that the interconnection term Δ_2 is bounded. For this purpose, from (43) and (44), we express the norm of Δ_2 as follows:

$$\|\Delta_2\|_2 = \frac{1}{m}|T_i|\,\|h_i\|_2 = \frac{1}{m}|T_i|\sqrt{h_{x_i}^2 + h_{y_i}^2 + h_{z_i}^2}. \tag{77}$$

Then, we leverage the following lemmas to show the boundedness of the coupling term Δ_2.

Lemma 4. *For a bounded desired trajectory (a_d, $\dot{a}_d$ and $\ddot{a}_d$) with $\|\ddot{a}_d\|_\infty = L_d$ and $\|\dot{a}_d\|_\infty = \bar{L}_d$, there exist finite positive constants c_{T_i} and k_{T_i} such that the trust feedback T_i satisfies the following property:*

$$\begin{aligned} &|T_i| \le k_{T_i}\left\|\begin{bmatrix} e_a \\ \dot{e}_a\end{bmatrix}\right\|_\infty, \ \textit{for} \left\|\begin{bmatrix} e_a \\ \dot{e}_a\end{bmatrix}\right\|_\infty \ge c_{T_i} \\ &|T_i| \le k_{T_i} c_{T_i}, \qquad \textit{for} \left\|\begin{bmatrix} e_a \\ \dot{e}_a\end{bmatrix}\right\|_\infty < c_{T_i} \end{aligned} \tag{78}$$

Proof. Letting $T = [T_1, \cdots, T_N]^{\mathrm{T}}$, $e_3 = [0, 0, 1]^{\mathrm{T}}$, and using (30) and (35), we have

$$\begin{aligned} \|T\|_\infty &= \max_{i=1,\cdots,N}(m\,\|v_i - g e_3\|_\infty) \\ &\le \max_{i=1,\cdots,N} m\,\|v_i\|_\infty + \max_{i=1,\cdots,N} mg \\ &\le mg + m\,\|v\|_\infty \\ &\le mg + m\left\|\beta^{\#}\right\|_\infty \Big(\|\ddot{a}_d\|_\infty + k_d\,\|\dot{e}_a\|_\infty + \\ &\qquad k_p\,\|e_a\|_\infty\Big) \\ &\le mg + m\hat{\beta}(L_d + k_d\,\|\dot{e}_a\|_\infty + \\ &\qquad k_p\,\|e_a\|_\infty) \\ &\le mg + m\hat{\beta}L_d + \\ &\qquad m\hat{\beta}\max(k_d, k_p)(\|\dot{e}_a\|_\infty + \|e_a\|_\infty), \\ &\le mg + m\hat{\beta}L_d + \\ &\qquad m\hat{\beta}\sqrt{2}\max(k_d, k_p)\left\|\begin{bmatrix} e_a \\ \dot{e}_a\end{bmatrix}\right\|_\infty \\ &\le m\hat{\beta}\sqrt{2}\max(k_d, k_p)\Bigg(\frac{mg + m\hat{\beta}L_d}{m\hat{\beta}\sqrt{2}\max(k_d, k_p)} + \\ &\qquad \left\|\begin{bmatrix} e_a \\ \dot{e}_a\end{bmatrix}\right\|_\infty\Bigg). \end{aligned} \tag{79}$$

Then, from (79), we can conclude that

$$\begin{aligned} |T_i| &\le \|T\|_\infty \\ &\le m\hat{\beta}\sqrt{2}\max(k_d, k_p)\Bigg(\frac{mg + m\hat{\beta}L_d}{m\hat{\beta}\sqrt{2}\max(k_d, k_p)} + \\ &\qquad \left\|\begin{bmatrix} e_a \\ \dot{e}_a\end{bmatrix}\right\|_\infty\Bigg) \\ &\le k_{T_i}\left(c_{T_i} + \left\|\begin{bmatrix} e_a \\ \dot{e}_a\end{bmatrix}\right\|_\infty\right). \end{aligned} \tag{80}$$

From (80), we can easily deduce the results in (78) by letting $k_{T_i} = 2m\hat{\beta}\sqrt{2}\max(k_d, k_p)$ and $c_{T_i} = \frac{mg + m\hat{\beta}L_d}{m\hat{\beta}\sqrt{2}\max(k_d, k_p)}$. □

Lemma 5. *There exist a positive constant c_{T_i} and a class$-\mathcal{K}$ function $\Gamma(.)$, such that the interconnection term Δ_2 satisfies the following condition:*

$$\|\Delta_2\|_2 \le \Gamma(\|e_\eta\|_2)\left\|\begin{bmatrix} e_a \\ \dot{e}_a\end{bmatrix}\right\|_\infty, \ \textit{for} \left\|\begin{bmatrix} e_a \\ \dot{e}_a\end{bmatrix}\right\|_\infty \ge c_{T_i} \tag{81}$$

Proof. Recalling (44), we first show that $\|h_i\|_2$ is bounded. For this purpose, we use the following inequalities

$$\begin{aligned} &|\sin\alpha| \le |\alpha|, |\cos\alpha| \le 1, |a||b| \le \frac{1}{2}(|a| + |b|), \\ &|a||b||c| \le \frac{1}{3}(|a| + |b| + |c|), \end{aligned} \tag{82}$$

for $|a| \le 1$, $|b| \le 1$, and $|c| \le 1$. Based on this, we have

$$\begin{aligned} |h_{1_i}| = |h_{3_i}| &\le |\sin(e_{\phi_i}/2)| \le 0.5|e_{\phi_i}|, \\ |h_{2_i}| = |h_{6_i}| &\le |\sin(e_{\theta_i}/2)| \le 0.5|e_{\theta_i}|, \\ |h_{4_i}| = |h_{5_i}| &\le |\sin(e_{\psi_i}/2)| \le 0.5|e_{\psi_i}|. \end{aligned} \tag{83}$$

Using (82) and (83), we have

$$\begin{aligned} |h_{x_i}| &\le \frac{23}{6}|\sin(e_{\phi_i}/2)| + \frac{7}{3}|\sin(e_{\theta_i}/2)| + \\ &\qquad \frac{23}{6}|\sin(e_{\psi_i}/2)| \\ &\le \frac{23}{6}(e_{\phi_i} + e_{\theta_i} + e_{\psi_i}), \\ |h_{y_i}| &\le \frac{23}{6}|\sin(e_{\phi_i}/2)| + \frac{7}{3}|\sin(e_{\theta_i}/2)| + \\ &\qquad \frac{23}{6}|\sin(e_{\psi_i}/2)| \\ &\le \frac{23}{6}(e_{\phi_i} + e_{\theta_i} + e_{\psi_i}), \\ |h_{z_i}| &\le \frac{3}{2}(|\sin(e_{\phi_i}/2)| + |\sin(e_{\theta_i}/2)|) \\ &\le \frac{3}{4}(e_{\phi_i} + e_{\theta_i}). \end{aligned} \tag{84}$$

From (84), we have $|h_{x_i}|^2 \le \frac{529}{9}(e_{\phi_i}^2 + e_{\theta_i}^2 + e_{\psi_i}^2)$, $|h_{y_i}|^2 \le \frac{529}{9}(e_{\phi_i}^2 + e_{\theta_i}^2 + e_{\psi_i}^2)$, and $|h_{z_i}|^2 \le \frac{9}{8}(e_{\phi_i}^2 + e_{\theta_i}^2)$, which results in

$$\begin{aligned} \|h_i\|_2 &\le \sqrt{\frac{1069}{9}(e_{\phi_i}^2 + e_{\theta_i}^2 + e_{\psi_i}^2)} \\ &\le 11\sqrt{e_{\phi_i}^2 + e_{\theta_i}^2 + e_{\psi_i}^2}. \end{aligned} \tag{85}$$

This article has been accepted for publication in IEEE Internet of Things Journal. This is the author's version which has not been fully edited and content may change prior to final publication. Citation information: DOI 10.1109/JIOT.2023.3305610

Quadcopter parameters			
Parameter name	Symbol	Value	Unit
Mass	m	0.34	Kg
Moment of inertia	I_{xx}	$3.22 * 10^{-4}$	Kgm^2
Moment of inertia	I_{xy}	0	Kgm^2
Moment of inertia	I_{xz}	0	Kgm^2
Moment of inertia	I_{yy}	3.0610^{-4}	Kgm^2
Moment of inertia	I_{yz}	0	Kgm^2
Moment of inertia	I_{zz}	$5.78 * 10^{-4}$	Kgm^2
Arm length	l	0.089	m

TABLE II: Quadcopter parameters

Controller and consensus parameters					
Symbol	Value	Symbol	Value	Symbol	Value
k_{p_1}	0.5	k_{d_1}	0.5	k_{ad_1}	34.2
k_{p_2}	0.5	k_{d_2}	0.5	k_{ad_2}	34.2
k_{p_3}	1.75	k_{d_3}	1.75	k_{ad_3}	22.8
k_{p_4}	0.15	k_{d_4}	0.15	k_{ap_1}	324
k_{p_5}	0.15	k_{d_5}	0.15	k_{ap_2}	324
k_{p_6}	0.15	k_{d_6}	0.15	k_{ap_3}	144
k_{p_7}	0.5	k_{d_7}	0.5	ρ	7.29
k_{p_8}	0.5	k_{d_8}	0.5	c	2
k_{p_9}	0.5	k_{d_9}	0.5		

TABLE III: Controller and consensus parameters

Ref. NO	Mean control	Heading control	Shape control	Setting	Model
Ours	Yes	Yes	Yes	Distributed	6-DOF Dynamic
[12]	Yes	No	No	Distributed	6-DOF Dynamic
[21]	Yes	No	No	Distributed	Double integrator
[28]	Yes	No	No	Centralized	6-DOF Dynamic
[29]	Yes	No	No	Distributed	6-DOF Dynamic
[30]	Yes	Yes	Yes	Centralized	Double integrator
[32]	Yes	Yes	Yes	Centralized	Double integrator
[33]	Yes	Yes	Yes	Distributed	Double integrator
[36]	Yes	Yes	Yes	Distributed	Double integrator
[39]	Yes	No	No	Distributed	Double integrator

TABLE IV: The comparison between the proposed framework and state-of-the-art swarm control methods.

Now, for $\left\| \begin{bmatrix} e_a \\ \dot{e}_a \end{bmatrix} \right\|_\infty \geq c_{T_i}$, we have

$$|T_i| \left\| h_i \right\|_2 \leq c_{\Delta_2} k_{T_i} \left\| e_\eta \right\|_2 \left\| \begin{bmatrix} e_a \\ \dot{e}_a \end{bmatrix} \right\|_\infty, \tag{86}$$

where $c_{\Delta_2} = 11$ and $\left\| e_\eta \right\|_2 = \sqrt{e_{\phi_i}^2 + e_{\theta_i}^2 + e_{\psi_i}^2}$. Further,

$$\left\| \Delta_2 \right\|_2 = \frac{1}{m} \left\| T_i h_i \right\|_2 \leq \Gamma(\left\| e_\eta \right\|_2) \left\| \begin{bmatrix} e_a \\ \dot{e}_a \end{bmatrix} \right\|_\infty, \tag{87}$$

where $\Gamma(\left\| e_\eta \right\|_2) = \frac{c_{\Delta_2}}{m} \left\| e_\eta \right\|_2$. □

Now, we state the stability of the overall closed loop system as follows:

Theorem 2. *For the swarm of quadcopters with strongly connected bidirectional graph $\mathcal{G}(t)$ and the swarm descriptors estimator in (19), with the proposed cooperative motion control law in (30) and attitude control law in (37), the collective motion of the swarm of quadcopters is asymptotically stable.*

Proof. The asymptotic stability of cascade systems can be ensured by showing all the system trajectories are bounded. To show the boundedness of system trajectories, it is sufficient to (1) show the stability of each of the systems, and (2) prove the boundedness of the interconnection terms [43], [44]. Based on this, the stability of cascade systems in (43) can be ensured if the designed control laws (30) and (37) are stable and the interconnection terms Δ_1 and Δ_2 are bounded. From Proposition 1, the control laws in (30 and 37) exponentially stabilizes the closed loop system in (43). Based on Corollary 4 and Lemma 5, the interconnection terms Δ_1 and Δ_2 are bounded. Therefore, it can be concluded that the overall system's trajectories are bounded. □

V. Flight Simulation Results

To demonstrate the performance of our collective motion framework for swarm of quadcopters, we have performed flight simulation experiments with various scenarios. Here, we present results that demonstrate the autonomous collective motion maneuvers including collective expansion, contraction, take-off, trajectory tracking, and landing. For this purpose, we consider a robotic swarm with nine identical quadcopters with parameters given in [49] and summarized in Table II for quadcopters' model given in (5) and (6). We assume that the quadcopters are initially located at $(0, 0, 10)$, $(0, 2, 0)$, $(0, 4, 0)$, $(2, 0, 0)$, $(2, 2, 0)$, $(2, 4, 0)$, $(4, 0, 0)$, $(4, 2)$, $(4, 4)$, and the underlying communication graph remains connected at all times. Also, we assume that $Quadcopter- 2$ crashes at time instant $t = 30sec$ to analyze the effect of robot drop-outs on the performance of the swarm.

In this flight simulation test, we command the swarm of quadcopters to navigate along a given path while controlling its heading, length, and width to a desired value. We provide the desired trajectory as follows: $\mu_{d_x} = t + 4$, $\mu_{d_y} = 0$, $\mu_{d_z} = 5\tanh(-t + 300) - \tanh(-t)$, $\theta_{d_x} = 0$, $\theta_{d_y} = 0$, $\theta_{d_z} = 0$, $s_{d_l} = 10$, $s_{d_w} = 8 + 4\sin(2\pi t/200)$, $s_{d_h} = 0$. To track the desired trajectory, we tune the controller and consensus parameters as shown in Table III. The results of collective navigation along the provided path is plotted in Figures 4 and 5. Figures 4a and 4b show the snapshot of collective motion of quadcopter swarm. To further investigate the history of the swarm's configuration, the swarm descriptors trajectory tracking results are plotted in Figure 5. Further, in Figure 6, we plot the control inputs to individual quadcopters in the swarm. From the flight simulation results, it can be observed that the swarm of quadcopters are attaining the desired collective motions while navigating along the given path in the presence of a robot dropout and communication link failures. Furthermore, we summarized the comparison between our proposed quadcopter swarm control framework to state-of-the-art frameworks as shown in Table IV. The comparison in Table IV shows the effectiveness of our proposed framework in the distributed collective motion of a swarm of quadcopters.

VI. Conclusion and Future Works

In this paper, we proposed a scalable and distributed control framework for collective navigation of swarm of quadcopters subjected robot drop-outs, and inter-robot communication link failures. The proposed quadcopter swarm control framework employed tools from abstraction and consensus theory to control the distribution of the swarm and stabilize the dynamics of the quadcopters. We proved that the framework guarantees

This article has been accepted for publication in IEEE Internet of Things Journal. This is the author's version which has not been fully edited and content may change prior to final publication. Citation information: DOI 10.1109/JIOT.2023.3305610

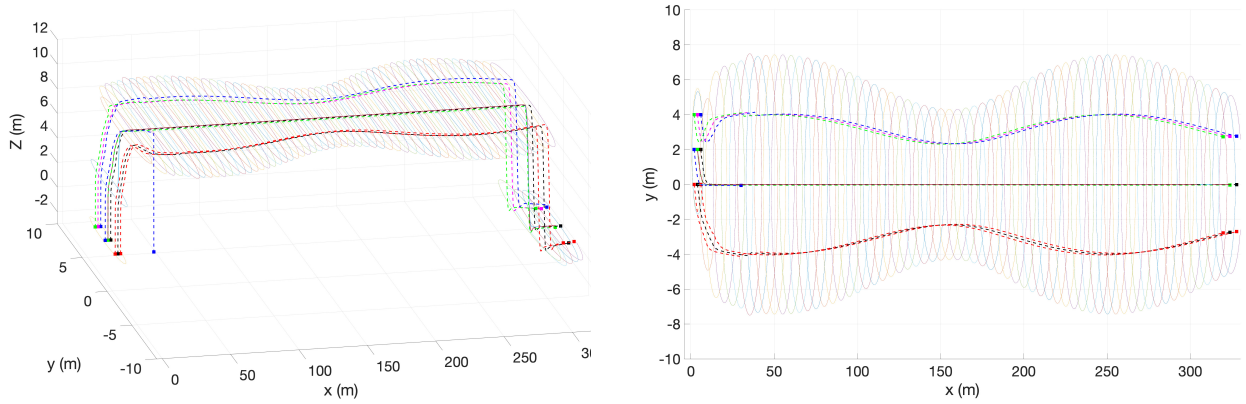

(a) 3-D view navigation of swarm of robots.

(b) Top view of navigation of swarm of robots.

Fig. 4: Navigation of swarm of robots along the desired path in 3-D space. The robots are initially in a square formation. Their formation evolves to rectangular and parallelogram shapes along the path.

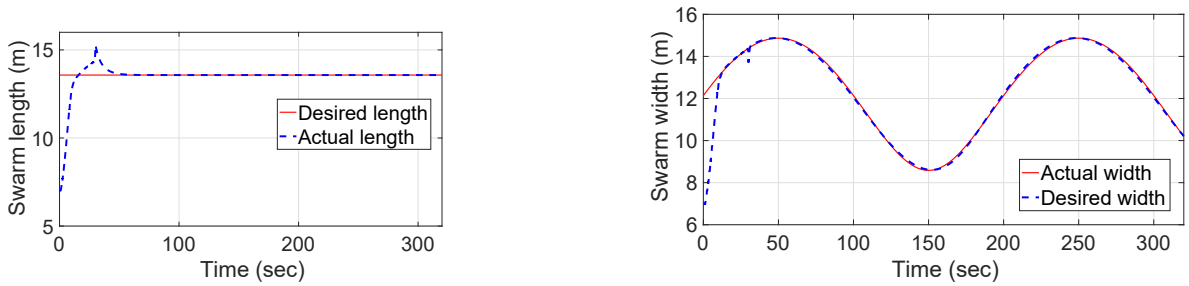

(a) Swarm length

(b) Swarm width

Fig. 5: Swarm width and swarm length tracking

realization of the desired collective maneuvers captured by the time-varying trajectory of the swarm descriptors. We also provided flight simulation results to evaluate the theoretical results and demonstrate the performance of the developed swarm control framework. Future research efforts focus on analyzing the effect of limited bandwidth capacity and noisy communication channels between adjacent robots, and hardware implementation of the proposed framework. Another future research direction for this work would be exploring the impact of inaccurate performance of UAVs' state estimator on the swarm descriptors estimation and control.

ACKNOWLEDGMENT

The authors would like to acknowledge the support from NSF under the award number 1832110, Sandia National Laboratories under Agreement number 2086781, and Air Force Research Laboratory and OSD for sponsoring this research under agreement number FA8750-15-2-0116.

REFERENCES

[1] R. Rajamani, H.-S. Tan, B. K. Law, and W.-B. Zhang, "Demonstration of integrated longitudinal and lateral control for the operation of automated vehicles in platoons," *IEEE Transactions on Control Systems Technology*, vol. 8, no. 4, pp. 695–708, 2000.

[2] K.-K. Oh, M.-C. Park, and H.-S. Ahn, "A survey of multi-agent formation control," *Automatica*, vol. 53, pp. 424–440, 2015.

[3] Y. Zheng, Q. Wang, D. Cao, B. Fidan, and C. Sun, "Distance-based formation control for multi-lane autonomous vehicle platoons," *IET Control Theory & Applications*, vol. 15, no. 11, pp. 1506–1517, 2021.

[4] X. Zhao, Y. Chen, and H. Zhao, "Robust approximate constraint-following control for autonomous vehicle platoon systems," *Asian Journal of Control*, vol. 20, no. 4, pp. 1611–1623, 2018.

[5] Q. Sun, X. Wang, G. Yang, Y.-H. Chen, and F. Ma, "Adaptive robust formation control of connected and autonomous vehicle swarm system based on constraint following," *IEEE transactions on cybernetics*, 2022.

[6] M. Cai, Q. Xu, C. Chen, J. Wang, K. Li, J. Wang, and X. Wu, "Formation control with lane preference for connected and automated vehicles in multi-lane scenarios," *Transportation research part C: emerging technologies*, vol. 136, p. 103513, 2022.

[7] M. Cai, Q. Xu, C. Chen, J. Wang, K. Li, J. Wang, and Q. Zhu, "Formation control for connected and automated vehicles on multi-lane roads: Relative motion planning and conflict resolution," *IET Intelligent Transport Systems*, vol. 17, no. 1, pp. 211–226, 2023.

[8] S. E. Li, Y. Zheng, K. Li, Y. Wu, J. K. Hedrick, F. Gao, and H. Zhang, "Dynamical modeling and distributed control of connected and automated vehicles: Challenges and opportunities," *IEEE Intelligent Transportation Systems Magazine*, vol. 9, no. 3, pp. 46–58, 2017.

[9] C. Ju and H. I. Son, "A distributed swarm control for an agricultural multiple unmanned aerial vehicle system," *Proceedings of the Institution of Mechanical Engineers, Part I: Journal of Systems and Control Engineering*, vol. 233, no. 10, pp. 1298–1308, 2019.

[10] V. Trianni, J. IJsselmuiden, and R. Haken, "The saga concept: Swarm robotics for agricultural applications," Technical Report. 2016. Available online: http://laral. istc. cnr. it/saga . . . , Tech. Rep., 2016.

[11] D. Albani, J. IJsselmuiden, R. Haken, and V. Trianni, "Monitoring and mapping with robot swarms for agricultural applications," in *2017 14th*

This article has been accepted for publication in IEEE Internet of Things Journal. This is the author's version which has not been fully edited and content may change prior to final publication. Citation information: DOI 10.1109/JIOT.2023.3305610

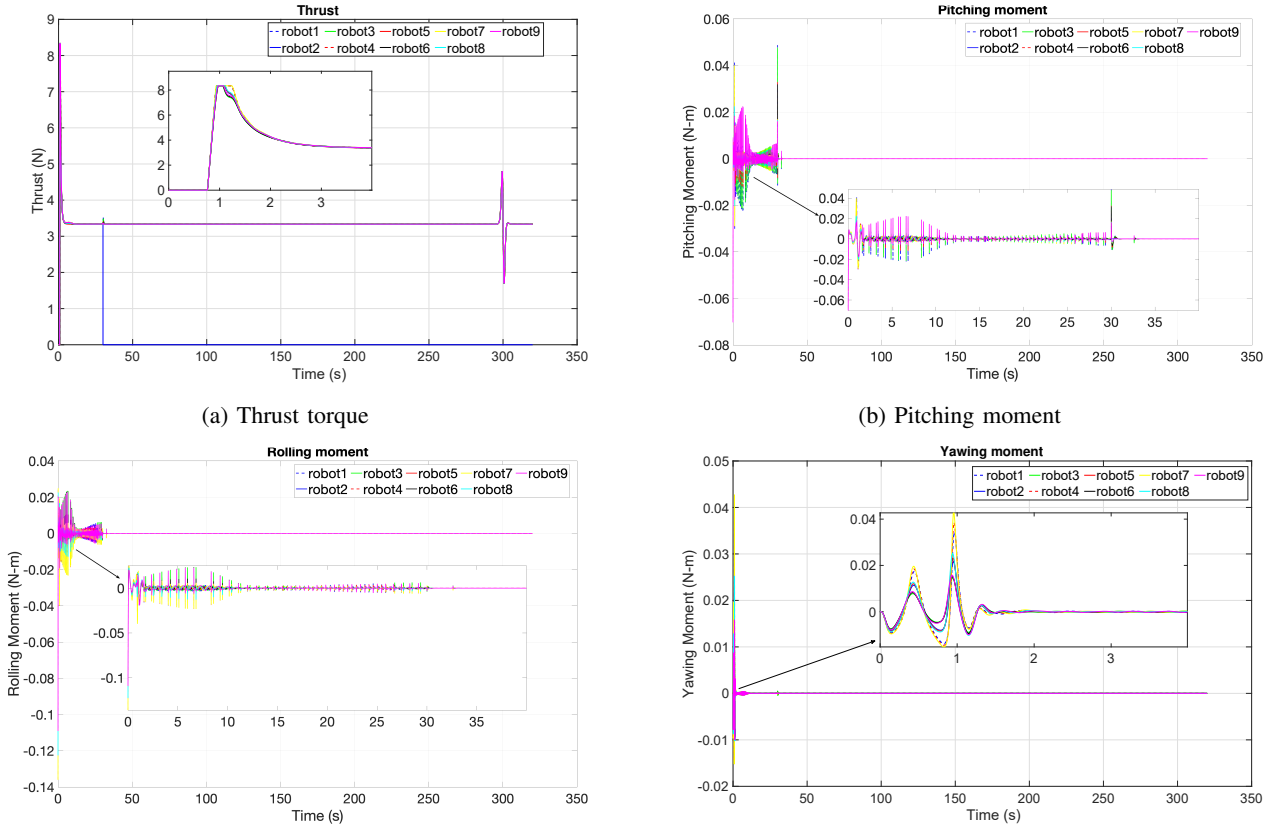

(a) Thrust torque

(b) Pitching moment

(c) Rolling moment

(d) Yawing moment

Fig. 6: Control input to each robot in the swarm.

IEEE International Conference on Advanced Video and Signal Based Surveillance (AVSS). IEEE, 2017, pp. 1–6.

[12] B. Shirani, M. Najafi, and I. Izadi, "Cooperative load transportation using multiple uavs," *Aerospace Science and Technology*, vol. 84, pp. 158–169, 2019.

[13] L. Ruan, G. Li, W. Dai, S. Tian, G. Fan, J. Wang, and X. Dai, "Cooperative relative localization for uav swarm in gnss-denied environment: A coalition formation game approach," *IEEE Internet of Things Journal*, 2021.

[14] N. Nigam, S. Bieniawski, I. Kroo, and J. Vian, "Control of multiple uavs for persistent surveillance: Algorithm and flight test results," *IEEE Transactions on Control Systems Technology*, vol. 20, no. 5, pp. 1236–1251, 2011.

[15] L. Zhou, S. Leng, Q. Liu, and Q. Wang, "Intelligent uav swarm cooperation for multiple targets tracking," *IEEE Internet of Things Journal*, vol. 9, no. 1, pp. 743–754, 2021.

[16] M. Brambilla, E. Ferrante, M. Birattari, and M. Dorigo, "Swarm robotics: a review from the swarm engineering perspective," *Swarm Intelligence*, vol. 7, no. 1, pp. 1–41, 2013.

[17] J. R. Lawton, R. W. Beard, and B. J. Young, "A decentralized approach to formation maneuvers," *IEEE transactions on robotics and automation*, vol. 19, no. 6, pp. 933–941, 2003.

[18] J. Seo, Y. Kim, S. Kim, and A. Tsourdos, "Consensus-based reconfigurable controller design for unmanned aerial vehicle formation flight," *Proceedings of the Institution of Mechanical Engineers, Part G: Journal of Aerospace Engineering*, vol. 226, no. 7, pp. 817–829, 2012.

[19] Z. Li, X. Xing, and J. Yu, "Decentralized output-feedback formation control of multiple 3-dof laboratory helicopters," *Journal of the Franklin Institute*, vol. 352, no. 9, pp. 3827–3842, 2015.

[20] B. Zhu, H. H.-T. Liu, and Z. Li, "Robust distributed attitude synchronization of multiple three-dof experimental helicopters," *Control Engineering Practice*, vol. 36, pp. 87–99, 2015.

[21] X. Wang, V. Yadav, and S. Balakrishnan, "Cooperative uav formation flying with obstacle/collision avoidance," *IEEE Transactions on control systems technology*, vol. 15, no. 4, pp. 672–679, 2007.

[22] A. Karimoddini, H. Lin, B. M. Chen, and T. H. Lee, "Hybrid three-dimensional formation control for unmanned helicopters," *Automatica*, vol. 49, no. 2, pp. 424–433, 2013.

[23] M. Radmanesh and M. Kumar, "Flight formation of uavs in presence of moving obstacles using fast-dynamic mixed integer linear programming," *Aerospace Science and Technology*, vol. 50, pp. 149–160, 2016.

[24] A. Mahmood and Y. Kim, "Leader-following formation control of quadcopters with heading synchronization," *Aerospace Science and Technology*, vol. 47, pp. 68–74, 2015.

[25] V. Roldão, R. Cunha, D. Cabecinhas, C. Silvestre, and P. Oliveira, "A leader-following trajectory generator with application to quadrotor formation flight," *Robotics and Autonomous Systems*, vol. 62, no. 10, pp. 1597–1609, 2014.

[26] C. Hua, J. Chen, and Y. Li, "Leader-follower finite-time formation control of multiple quadrotors with prescribed performance," *International Journal of Systems Science*, vol. 48, no. 12, pp. 2499–2508, 2017.

[27] E. Zhao, T. Chao, S. Wang, and M. Yang, "Finite-time formation control for multiple flight vehicles with accurate linearization model," *Aerospace Science and Technology*, vol. 71, pp. 90–98, 2017.

[28] W. Jasim and D. Gu, "Robust team formation control for quadrotors," *IEEE Transactions on Control Systems Technology*, vol. 26, no. 4, pp. 1516–1523, 2017.

[29] H. Liu, T. Ma, F. L. Lewis, and Y. Wan, "Robust formation control for multiple quadrotors with nonlinearities and disturbances," *IEEE transactions on cybernetics*, vol. 50, no. 4, pp. 1362–1371, 2018.

[30] C. Belta and V. Kumar, "Abstraction and control for groups of robots," *IEEE Transactions on robotics*, vol. 20, no. 5, pp. 865–875, 2004.

[31] S. Shahrokhi, L. Lin, C. Ertel, M. Wan, and A. T. Becker, "Steering a swarm of particles using global inputs and swarm statistics," *IEEE Transactions on Robotics*, vol. 34, no. 1, pp. 207–219, 2017.

[32] K. L. Crandall and A. Wickenheiser, "Controlling parent systems through swarms using abstraction," *IEEE Transactions on Control of Network Systems*, 2019.

[33] P. Yang, R. A. Freeman, and K. M. Lynch, "Multi-agent coordination by

decentralized estimation and control," *IEEE Transactions on Automatic Control*, vol. 53, no. 11, pp. 2480–2496, 2008.

[34] R. A. Freeman, P. Yang, and K. M. Lynch, "Distributed estimation and control of swarm formation statistics," in *2006 American Control Conference*. IEEE, 2006, pp. 7–pp.

[35] S. Gudeta, A. Karimoddini, M. Davoodi, and I. Raptis, "Leaderless swarm formation control: From global specifications to local control laws," in *2021 American Control Conference (ACC)*. IEEE, 2021, pp. 808–813.

[36] C. J. Stamouli, C. P. Bechlioulis, and K. J. Kyriakopoulos, "Multi-agent formation control based on distributed estimation with prescribed performance," *IEEE Robotics and Automation Letters*, vol. 5, no. 2, pp. 2929–2934, 2020.

[37] S. Gudeta, A. Karimoddini, and M. Davoodi, "Robust dynamic average consensus for a network of agents with time-varying reference signals," in *2020 IEEE International Conference on Systems, Man, and Cybernetics (SMC)*. IEEE, 2020, pp. 1368–1373.

[38] X. Dong, Y. Zhou, Z. Ren, and Y. Zhong, "Time-varying formation tracking for second-order multi-agent systems subjected to switching topologies with application to quadrotor formation flying," *IEEE Transactions on Industrial Electronics*, vol. 64, no. 6, pp. 5014–5024, 2016.

[39] X. Dong, Y. Li, C. Lu, G. Hu, Q. Li, and Z. Ren, "Time-varying formation tracking for uav swarm systems with switching directed topologies," *IEEE transactions on neural networks and learning systems*, vol. 30, no. 12, pp. 3674–3685, 2018.

[40] J. George and R. A. Freeman, "Robust dynamic average consensus algorithms," *IEEE Transactions on Automatic Control*, vol. 64, no. 11, pp. 4615–4622, 2019.

[41] A. Marsden, "Eigenvalues of the laplacian and their relationship to the connectedness of a graph," *University of Chicago, REU*, 2013.

[42] J. George, R. A. Freeman, and K. M. Lynch, "Robust dynamic average consensus algorithm for signals with bounded derivatives," in *2017 American Control Conference (ACC)*. IEEE, 2017, pp. 352–357.

[43] I. Fantoni, R. Lozano, and F. Kendoul, "Asymptotic stability of hierarchical inner-outer loop-based flight controllers," *IFAC Proceedings Volumes*, vol. 41, no. 2, pp. 1741–1746, 2008.

[44] F. Kendoul, Z. Yu, and K. Nonami, "Guidance and nonlinear control system for autonomous flight of minirotorcraft unmanned aerial vehicles," *Journal of Field Robotics*, vol. 27, no. 3, pp. 311–334, 2010.

[45] E. D. Sontag *et al.*, "Smooth stabilization implies coprime factorization," *IEEE transactions on automatic control*, vol. 34, no. 4, pp. 435–443, 1989.

[46] R. Horn and C. Johnson, "Matrix analysis, 2nd edn cambridge," *UK: Cambridge University Press.[Google Scholar]*, 2013.

[47] F. Chen, Y. Cao, and W. Ren, "Distributed average tracking of multiple time-varying reference signals with bounded derivatives," *IEEE Transactions on Automatic Control*, vol. 57, no. 12, pp. 3169–3174, 2012.

[48] K. Scaman, F. Bach, S. Bubeck, Y. T. Lee, and L. Massoulié, "Optimal algorithms for smooth and strongly convex distributed optimization in networks," in *international conference on machine learning*. PMLR, 2017, pp. 3027–3036.

[49] B. Prabhakaran, M. Kothari *et al.*, "Nonlinear control design for quadrotors," in *2015 IEEE workshop on computational intelligence: Theories, applications and future directions (WCI)*. IEEE, 2015, pp. 1–6. [Online]. Available: https://github.com/Prabhu-369/Control-algorithm-for-quadcopter

Solomon G. Gudeta received his B.Sc. degree in Electrical Engineering from the Bahir Dar University, Ethiopia, in 2010. He later received his M.Sc. degree in Mechatronics Engineering with specialization in Robotics from the University of Trento in 2015, and the Ph.D. degree from the Department of Electrical Engineering at the North Carolina A&T State University in 2021. He is a member of utonomous Cooperative Control of Emergent Systems of Systems (ACCESS) Laboratory at NCA&T State University. His research interests include control of multi-agent systems and robotic swarms, motion planning and control of autonomous vehicles, aerial robotics, and flight control systems.

Ali Karimoddini (Senior Member, IEEE) is a Professor in the ECE Department at the North Carolina A&T State University. He received the Bachelor of Electrical and Electronics Engineering degree from the Amirkabir University of Technology, Iran, in 2003, the Master of Science degree in instrumentation and automation engineering from the Petroleum University of Technology in 2007, and the Ph.D. degree in electrical engineering from the National University of Singapore, Singapore, in 2013. His research interests include control and robotics, autonomy, resilient control systems, smart transportation, connected and autonomous vehicles, human–machine interactions, cyber-physical systems, flight control systems, and multi-agent systems. He is the Director of CR^2C^2 Regional University Transportation Center, the Director of the NC-CAV Center of Excellence on Advanced Transportation Technology, and the Director of the ACCESS Laboratory.

Negasa Yahi received his B.Sc. degree in Electrical and computer Engineering and M.Sc. in Control and Instrumentation Engineering from Jimma University, Ethiopia in 2016 and 2019, respectively. He is currently working towards his Ph.D. in Electrical Engineering in the North Carolina A&T State University. He is a member of utonomous Cooperative Control of Emergent Systems of Systems (ACCESS) Laboratory at NCA&T State University. His research interests include Urban Air Mobility, tasking and path planning for UAVs, and flight control systems.